

**Conditional Stomatal Closure in a Fern
Shares Molecular Features with
Flowering Plant Active Stomatal Responses**

**Andrew R.G. Plackett^{1,3,4*}, David M. Emms¹, Steven Kelly¹, Alistair M. Hetherington², Jane A.
Langdale¹**

¹ University of Oxford, Department of Plant Sciences, South Parks Road, Oxford, Oxfordshire, OX1
3RB, UK

² University of Bristol, School of Biological Sciences, 24 Tyndall Avenue, Bristol, BS8 1TQ, UK

³ Present address: University of Birmingham, School of Biosciences, Edgbaston, Birmingham, West
Midlands, B15 2TT, UK

⁴Lead contact

*Correspondence: A.R.G.Plackett@bham.ac.uk

Twitter: @SeedEvolution

SUMMARY

Stomata evolved as plants transitioned from water to land, enabling carbon dioxide uptake and water loss to be controlled. In flowering plants, the most recently divergent land plant lineage, stomatal pores actively close in response to drought. In this response, the phytohormone abscisic acid (ABA) triggers signalling cascades that lead to ion and water loss in the guard cells of the stomatal complex, causing a reduction in turgor and pore closure. Whether this stimulus-response coupling pathway acts in other major land plant lineages is unclear, with some investigations reporting that stomatal closure involves ABA but others concluding that closure is passive. Here we show that in the model fern *Ceratopteris richardii* active stomatal closure is conditional on sensitisation by pre-exposure to either low humidity or exogenous ABA and is promoted by ABA. RNA-seq analysis and *de novo* transcriptome assembly reconstructed the protein coding complement of the *C. richardii* genome with coverage comparable to other plant models, enabling transcriptional signatures of stomatal sensitisation and closure to be inferred. In both cases, changes in abundance of homologs of ABA, Ca²⁺ and ROS-related signalling components were observed, suggesting that the closure response pathway is conserved in ferns and flowering plants. These signatures further suggested that sensitisation is achieved by lowering the threshold required for a subsequent closure-inducing signal to trigger a response. We conclude that the canonical signalling network for active stomatal closure functioned in at least a rudimentary form in the stomata of the last common ancestor of ferns and flowering plants.

Keywords: Evolution, stomata, ABA, fern, *Ceratopteris richardii*, RNA-seq

1 INTRODUCTION

2 Stomata are pores present on the surfaces of plant leaves that control the uptake of CO₂ and the loss
3 of water vapour. The acquisition of stomata was a key land plant adaptation, which together with the
4 development of a waxy cuticle and vascular system allowed early plants to colonise the terrestrial
5 environment¹. The ability to control CO₂ uptake is important in the context of photosynthesis, whereas
6 the regulation of evapotranspiratory water loss impacts on water and mineral nutrient accumulation in
7 the aerial parts of the plant, protects against short periods of reduced soil water availability and provides
8 leaf cooling capacity. Stomatal closure also provides protection against invasion by some pathogens.
9 The regulation of stomatal aperture by light, humidity, atmospheric CO₂, and the plant hormone
10 abscisic acid (ABA) has been extensively investigated in the model flowering plant *Arabidopsis*
11 *thaliana*. These studies identified networks of intracellular signalling proteins and second messengers
12 that act in stomatal guard cells to couple extracellular stimuli to an opening or closing response^{2,3,4}.
13 Although stomata are present in all land plant lineages except liverworts⁵, in which they have likely
14 been secondarily lost⁶, the question of when active stomatal closure mechanisms evolved remains
15 hotly debated.

16
17 Studies of stomatal responses in non-flowering plant species have led to conflicting interpretations of
18 underlying mechanisms. Observations that stomata close in response to ABA and CO₂ in two moss
19 species⁷, *in silico* evidence suggesting that stomata evolved only once⁶ and the presence of genes
20 encoding components of *Arabidopsis* stomatal closure pathways in moss genomes^{8,9} could indicate
21 that active stomatal responses are ancient. However, physiological experiments in two hornwort
22 species (a second stomata-bearing bryophyte lineage) found that their stomata were unresponsive to
23 ABA or desiccation¹⁰, and thus a bryophyte origin of active stomatal responses is contested. Reports
24 from non-flowering vascular plants have been similarly contradictory. Some suggest that in lycophytes
25 and ferns stomatal closure is hydropassive and guard cells are insensitive to closure-inducing signals
26 such as ABA and high CO₂ levels^{11,12,13,14,15} whilst in contrasting reports stomata in the lycophyte
27 *Selaginella uncinata*¹⁶ and a number of ferns^{9,17,18, 19,20,21} were shown to close in response to ABA
28 and/or CO₂. The observation that stomatal closure in response to exogenous ABA is conditional on
29 growth conditions in some (but not all) species of fern¹⁸ may highlight the confounding variable in

previous reports, but the underlying molecular basis for fern stomatal closure and conditional responsiveness is unknown.

To identify the pathways underlying fern stomatal closure mechanisms, we utilised RNA-seq technology and *de novo* transcript assembly to generate and compare entire transcriptome profiles associated with different stomatal responses in the fern *Ceratopteris richardii*. It has previously been suggested that stomatal closure in *C. richardii* is not activated by the canonical ABA-induced response pathway found in flowering plants, based on the observation that stomatal conductance is reduced in response to increased water vapour deficit even in a mutant lacking a functional homolog of a receptor kinase required for ABA-induced stomatal closure in *Arabidopsis*²². However, *C. richardii* is a neotropical semi-aquatic fern that is routinely grown at high humidity (i.e. low water vapour deficit) under laboratory conditions^{23,24}, and stomatal responses may have been masked by conditional behaviours now known from other ferns¹⁸. We demonstrate herein that the stomata of *C. richardii* can actively close in response to both low humidity and ABA, but this response is dependent on previous sensitisation by either low humidity or ABA. Our RNA-seq analysis provides evidence that the signalling network controlling stomatal closure in ferns contains homologs of ABA transport, Ca²⁺ signalling and ROS signalling components from canonical *Arabidopsis* stomatal closure pathways, and suggests that sensitisation potentiates these same pathways to respond to closure stimuli at a lower threshold. We conclude that a core of regulatory networks that control active stomatal closure is at least partially conserved between ferns and flowering plants.

RESULTS

Active stomatal closure in *C. richardii* is conditional on pre-sensitisation by low humidity or exogenous ABA

To test whether active stomatal closure in *C. richardii* is conditional on growth environment, stomatal responses were compared between two humidity pretreatments. Plants were grown either in constant high relative humidity ($94.9 \pm 0.36\%$) (hereafter 'wet-grown') or periodically exposed to low (ambient) humidity ($48.3 \pm 0.69\%$) (hereafter 'dry-pretreated') for ten minutes (see STAR Methods). After an interval of growth at high humidity to ensure all stomata were open, both pretreatment groups were

1 exposed to low humidity for 120 minutes. Stomata of fronds from dry-pretreated plants exhibited a
2 significant ($p < 0.05$) and progressive reduction in stomatal pore area in response to low humidity at
3 both 60 and 120 minutes (**Figure 1A**), with mean pore areas of 79.7% and 54.0% of the mean area
4 measured at 0 minutes, respectively (**Data S1A**). Simultaneous application of exogenous ABA
5 significantly enhanced this response ($p < 0.05$) at both 60 (66.9%) and 120 minutes (40.0%) (**Figure**
6 **1A**). In contrast, stomata of wet-grown plants showed a significantly reduced pore area ($p < 0.05$) only
7 after 120 minutes and of much lesser magnitude (89.0% of mean pore area at 0 minutes), with no
8 response to ABA ($p > 0.05$) (**Figure 1A**). Dry-pretreated plants exhibited a specific reduction in pore
9 aperture width and not length (**Figure S1**), with a greater resilience to wilting than wet-grown plants
10 without any change in stomatal density (**Figure S1**), supporting active closure. When assays were
11 repeated under constant high humidity stomatal responses of dry-pretreated plants were much
12 reduced, with mean pore area at 60 and 120 minutes 81.6% and 76.2% compared to 0 minutes and
13 no significant change between 60 and 120 minutes ($p > 0.05$) (**Figure 1B**), potentially a weak response
14 to a transient reduction in humidity during mock or ABA treatment application (see STAR Methods).
15 No response to exogenous ABA was detected under high humidity (**Figure 1B**). Stomata of wet-grown
16 plants also demonstrated a minor closure response under high humidity ($p < 0.05$) (**Figure 1B**), similar
17 in magnitude to their response under low humidity (**Data S1A**). *C. richardii* stomata of wet-grown plants
18 may therefore not be entirely insensitive to humidity, but dry pretreatment was necessary and sufficient
19 to significantly enhance stomatal active closure in response to a low humidity stimulus, and low
20 humidity was required to see any effect of an ABA stimulus on closure in sensitised stomata.

21
22 To test whether stomata could also be sensitised solely by ABA, wet-grown plants were pretreated with
23 periodic application of exogenous ABA or a mock solution (see STAR Methods). When subsequently
24 exposed to a low humidity stimulus, stomata from ABA-pretreated plants showed a significant reduction
25 in stomatal area compared to mock-pretreated controls ($p < 0.05$) at 60 and 120 minutes (**Figure 1C**),
26 achieving the same magnitude of closure by 60 minutes (51.1%) as in dry-pretreated plants by 120
27 minutes (**Data S1A**). Exogenous ABA treatment did not enhance this response further ($p > 0.05$, **Figure**
28 **1C**), presumably because maximum closure had already been reached. Stomata from mock-pretreated
29 plants were essentially unresponsive to low humidity, with a transient reduction in aperture area at 60

minutes only ($p < 0.05$) to 87.7% of mean pore area at 0 minutes (**Figure 1C**). ABA-pretreated plants showed greater resistance to wilting compared with controls with no change in stomatal density (**Figure S1**). When assayed under high humidity the closure responses of stomata from ABA-pretreated plants were lost ($p > 0.05$, **Figure 1D**), but exogenous ABA did elicit a minor response ($p < 0.05$) after 120 minutes (87.0%) (**Figure 1D, Data S1A**). Stomata from mock-pretreated plants exhibited a similar response to wet-pretreated plants under high humidity (**Figure 1B and 1D, Data S1A**). Together these results show *C. richardii* stomata can be sensitised by ABA without low humidity, enabling subsequent active closure in response to either low humidity or ABA.

Homologs of *Arabidopsis* regulators of stomatal aperture and ABA responses are differentially expressed during stomatal sensitisation in *C. richardii*

To identify genetic components of the mechanisms underlying stomatal sensitisation in *C. richardii*, RNA-seq was used to establish genome-wide transcript profiles in fronds of wet-grown, dry-pretreated, and ABA-pretreated plants (**Figure 2A**). The final *de novo* transcriptome assembled (see STAR Methods) contained 201,391 transcript isoforms corresponding to 107,173 genes, of which 106,828 transcripts (corresponding to 23,690 genes) were classified as expressed. The predicted proteome comprised 33,699 protein-coding transcripts, with at most one per gene. BUSCO analysis determined that this proteome was more complete than a published *C. richardii* partial genome assembly²⁵ and of similar completeness to published genomes for other plant species (**Figure 2B**) and another *de novo* *C. richardii* transcriptome sampling different tissue types (**Table S1**)²⁶. The total assembly contained a significant proportion of duplicated transcripts. Comparison with the predicted proteome indicates is predominantly due to the presence of isoforms (**Figure 2B**). The majority of protein-coding transcripts (68.7%) had identifiable homology to *Arabidopsis* genes (see STAR Methods), of which 49% were direct orthologs to *Arabidopsis* genes (**Figure 2C**). The quality of our *de novo* proteome was thus sufficient to identify conserved genetic networks between *Arabidopsis* and *C. richardii*.

Comparing transcriptome profiles between wet-grown (non-sensitised) and dry-pretreated or ABA-pretreated (sensitised) fronds revealed 67 transcripts with significantly different abundance levels ($p < 0.05$) in wet-grown versus dry-pretreated fronds and 6919 transcripts with significantly different levels

($p < 0.05$) in wet-grown versus ABA-pretreated fronds (**Figure 3A**). The large number of genes responding to ABA pretreatment was anticipated because there were pleiotropic effects on frond morphology (**Figure S1**) and ABA is known to impact on other processes unrelated to stomata. Only 47 transcripts displayed significant differences in abundance (44 at $p < 0.01$ in at least one pretreatment; 3 at $0.01 < p < 0.05$) in both wet-grown versus dry-pretreated and wet-grown versus ABA-pretreated comparisons (**Figure 3A**). These transcripts responded similarly to dry and ABA pretreatments, 11 with significantly higher levels in sensitised fronds and 36 with lower levels ($p < 0.05$) (**Figure 3B**), and thus represent the stomatal sensitisation signature in *C. richardii*.

To assess the likely function of sensitisation signature transcripts, homologs were identified, similarity to known proteins was determined, and gene ontology (GO) terms were assigned. Thirty of the 47 sequences had recognisable homologs: 18 to one or more *Arabidopsis* genes, eight had no recognisable homologs in *Arabidopsis* but had in the bryophytes *Physcomitrium patens* (three), *Marchantia polymorpha* (one) or both (four), and four had significant BLAST similarity to known proteins (**Data S2A**). Seventeen remaining transcripts had no significant similarity to known proteins. Within the GO terms assigned to *Arabidopsis* homologs of identifiable transcripts, 46% were associated with responses to biotic or abiotic stimuli, 43% were related to membranes, and 25% were transporters (**Data S2A**). Some identifiable transcripts have no known role in *Arabidopsis* stomatal responses, possibly reflecting evolutionarily divergent functions or the use of whole-frond RNA in this study, but nine out of the 18 *Arabidopsis* homologs have links to known stress response or stomatal mechanisms. Two sensitisation signature transcripts are homologous to gene families with annotations linked to ABA and stomata, respectively (**Data S2A**), both families encoding plasma membrane ABC transporters that regulate *Arabidopsis* stomatal aperture. Phylogenetic analysis (**Figure S2**) identified transcript TRINITY_DN94_c0_g1 as one of four most closely-related *C. richardii* homologs to ABCG subfamily protein AtABCG40/AtPDR12, a guard cell ABA transporter²⁷, and TRINITY_DN8731_c0_g1 as one of four *C. richardii* orthologs of ABCC subfamily protein AtMRP4, which regulates stomatal aperture either upstream or independently of ABA²⁸. Both transporters are strongly expressed in *Arabidopsis* guard cells^{27,28}. A third transcript (TRINITY_DN5406_c0_g1) is an ortholog of AtGRDP1, a negative regulator of ABA responses²⁹. The AtPDR12 and AtGRDP1 homologs are down-regulated in sensitised *C.*

richardii fronds whereas the AtMRP4 homolog is up-regulated (**Data S2A**). Other sensitisation signature transcripts include one DREB and two WRKY transcription factors, one peroxidase superfamily protein and two calcium-binding proteins (**Data S2A**) that could affect downstream stress response pathways³⁰ or guard cell signalling cascades². Although many transcripts in the sensitisation signature have no known homologs and may have species-specific functions in stomatal regulation, others are recognisable components associated with known stimulus-response signalling mechanisms that regulate stomatal closure in flowering plants.

Homologs of genes required for stomatal closure in *Arabidopsis* are associated with stomatal closure in *C. richardii*

To identify genes underlying fern stomatal closure mechanisms, transcript profiles were generated from fronds with different stomatal sensitivities before and 60 minutes after exposure to different humidity and ABA treatments (**Figures 2A** and **S3**). Four assays were carried out using dry-pretreated (sensitised) fronds: maintenance at high humidity with and without ABA treatment (no closure), exposure to low humidity (closure), and exposure to low humidity and ABA (enhanced closure). Further transcriptomes were generated from wet-grown (non-sensitised) and ABA-pretreated (sensitised) plants before and after exposure to low humidity (wet-grown - no closure; ABA-pretreated - closure). Transcripts with significantly different levels ($p < 0.01$) before and after each assay were identified (**Data S3A**). Notably, fewer transcripts were responsive to low humidity in ABA-pretreated fronds, possibly reflecting altered expression at timepoint 0 as a result of ABA pretreatment and/or more rapid stomatal closure than in dry-pretreated fronds (**Figure 1C**) precluded the capture of at least some changes underlying the closure mechanism. Transcripts specifically associated with stomatal closure were identified by comparing transcript profiles between assay pairs where stomata closed in one but not the other (**Figure S3**), comparing four pairs to filter out non-specific responses. 1858 transcripts showed a significant change in abundance ($p < 0.01$) specifically upon stomatal closure in at least one assay pair (**Figure S3**), of which four were detected in all four paired datasets, 141 in at least three datasets and 877 in at least two datasets (**Figure 4A**). Hereafter we refer to these 877 transcripts as stomatal closure-associated transcripts, and the 141 transcripts present in at least three datasets as the stomatal closure signature.

1
2 To determine whether any of the closure-associated transcripts are homologous to genes involved in
3 *Arabidopsis* stomatal closure networks, stomatal and ABA annotations were mapped onto the whole
4 transcriptome assembly (see STAR Methods). Fifty-one of the 877 transcripts had homology to
5 *Arabidopsis* genes with stomatal or ABA annotations, of which five were closure signature transcripts
6 (**Figure 4B**). To further investigate gene function, the 51 transcripts were screened for homology to 14
7 *Arabidopsis* genes with proven roles in stomatal closure^{2,31}, all of which had identifiable homologs
8 within the transcriptome assembly (**Table S2**). One of the five annotated signature transcripts was
9 homologous to the SHAKER family of gated potassium ion channels that function in the guard cell
10 membrane to effect stomatal closure³² (**Figure 4C**). The remaining 46 annotated closure-associated
11 transcripts include homologs of aquaporin, CPK calcium-dependent protein kinase, respiratory burst
12 oxidase homolog (RBOH) and annexin gene families (**Figure 4C** and **Data S3B**). Although no
13 canonical components of the ABA signal transduction pathway were found, two families of ABA influx
14 channels involved in stomatal closure were identified (**Figure 4C**). Homologs of genes in many of the
15 signalling pathways that mediate stomatal closure in *Arabidopsis* are thus associated with stomatal
16 closure in *C. richardii*, suggesting that closure mechanisms are at least partially conserved between
17 ferns and angiosperms.

18

19 **Changes in transcript abundance during stomatal closure and sensitisation in *C. richardii* are** 20 **largely ABA-independent**

21 To further dissect ABA-related mechanisms underlying stomatal closure in *C. richardii*, we exploited
22 the finding that stomata in dry-pretreated plants only respond to ABA when the ABA treatment is carried
23 out under low humidity conditions (**Figures 1A** and **1B**). ABA-related changes in transcript abundance
24 specific to stomatal closure should thus be observed following ABA treatment only under low humidity.
25 Transcripts responsive to ABA under low and high humidity were identified by comparing
26 transcriptomes of dry-pretreated fronds exposed to either a mock solution or ABA treatment at each
27 humidity level. 578 and 607 transcripts had significantly altered abundance ($p < 0.01$) in response to
28 ABA under low and high humidity, respectively (**Figure S4** and **Data S4A**). Two of the 141 closure
29 signature transcripts changed abundance after ABA treatment under high humidity (representing an

unknown protein and a UDP-glucose 6-dehydrogenase, **Data S4B**), but none were ABA-responsive under low humidity (**Figure 5A**) and only 13 closure-associated transcripts changed abundance in response to ABA specifically under low humidity (**Figure S4** and **Data S4B**). These results suggest that ABA-induced closure of fern stomata is mediated primarily via mechanisms operating at translational or post-translational levels.

Transcriptome profiles during stomatal sensitisation and closure in *C. richardii* suggest that sensitisation is associated with the down-regulation of closure-associated genes

To determine whether fern stomatal sensitisation and closure mechanisms are related, the identities of sensitisation signature transcripts were compared to those of closure-associated transcripts. Twenty four of the 47 sensitisation signature transcripts were present in the closure-associated transcript dataset, with two also closure signature transcripts (**Figure 5B**). Fourteen of these 24 transcripts have similarity to known proteins (**Data S3C**) and include the ABCG transporter homolog, the AtGRDP1 ortholog, the peroxidase superfamily protein and two calcium-binding EF-hand family proteins. Notably, all 24 transcripts decreased in abundance during sensitisation and increased in abundance during closure (**Figure 5C**), returning to levels similar to untreated wet-grown plants ($p > 0.05$) (**Figure 5D** and **Data S3C**). The fact that more than 50% of sensitisation signature transcripts represent stomatal closure-associated transcripts suggests that stomatal sensitisation acts by priming the closure mechanism.

DISCUSSION

Stomata facilitated the adaptation of plants to land and, with the exception of liverworts, all extant land plant lineages possess stomata with the capacity to open and close. In extant vascular plants stomata modulate the exchange of air and water with the surrounding environment but in mosses and hornworts they are instead proposed to mediate sporophyte desiccation^{10,33}. Despite the likely monophyletic origin of stomata the evolution of their regulatory networks is disputed, particularly whether the ABA-dependent active stomatal closure mechanisms found in flowering plants^{2,34} are conserved in non-flowering vascular plants. We show that stomatal closure in the fern *C. richardii* is active but is conditional on sensitisation by prior exposure to either low humidity or ABA. To identify the mechanisms

underlying these processes, we utilised RNA-seq to compare transcriptomes of whole fronds exposed to different conditions under which stomata did or did not close, and from these inferred putative signatures associated with stomatal responses. These suggest that both stomatal sensitisation and closure in *C. richardii* include transcriptional changes in signalling pathways conserved with active stomatal closure in the flowering plant *Arabidopsis*. Active stomatal closure responses are thus likely to have evolved in a land plant ancestor shared by all extant land plant groups.

Active stomatal closure mechanisms are conserved in ferns and flowering plants

The requirement for sensitisation to reveal active stomatal closure responses, shown here in *C. richardii* and previously in some other leptosporangiate fern species¹⁸, might reconcile past reports of non-active stomatal responses in basal land plant lineages^{11,12,13,14,15} but the extent to which conditional stomatal sensitivity is present across the fern lineage remains unclear. In *C. richardii* only sensitised stomata responded to ABA treatment, but ABA pretreatment was itself sufficient to cause stomatal sensitisation. Other ferns vary from stomata being ABA-responsive without prior sensitisation^{9,21} to no ABA response despite dry pretreatment¹⁸. This study used 100 μ M ABA, ten times that necessary in *Arabidopsis*¹⁸, following experiments with the lycophyte *Selaginella uncinata*¹⁶ and the fern *Nephrolepis exaltata*¹⁹ and to mitigate against dilution of the ABA signal in standing water within the environment (see STAR Methods). The stomata of some fern species respond to lower ABA concentrations (10-50 μ M ABA)^{9,18}, but others do not¹⁸. Although ABA content has been measured in *C. richardii* whole fronds²², the native concentration range specifically in fern guard cells is unknown and their sensitivity may differ from flowering plants. A recent study further indirectly supports active stomatal responses in ferns, showing that across the fern lineage stomata open in response to blue light³⁵ as in flowering plants³⁶. Our findings thus contribute to an emerging consensus that active regulation of stomatal responses is present across the fern lineage.

ABA induction of stomatal closure in *Arabidopsis* involves the canonical RCAR/PRY/PYL - PP2C ABA signal transduction complex^{34,37,38,39}, two well-characterised ABA responsive proteins (Snf1-Related Kinase subfamily 2 (SnRK2)⁴⁰ and S-type anion channels (SLAC)^{41,42}) and a number of downstream genes including those encoding ABA influx channels, calcium and ROS signalling components, and K⁺

ion channels². ABA treatment caused *C. richardii* stomata to close more rapidly under low humidity but no RCAR/PRY/PYL, SLAC or SnRK2 transcripts changed abundance. In contrast, A *SLAC1* homolog was identified as ABA-responsive in a qPCR study of another fern⁹. This discrepancy could relate to different experimental humidity conditions, which strongly altered *C. richardii* transcriptional responses to ABA. *Arabidopsis* stomatal SLAC channel activity is activated post-transcriptionally by ABA via SnRK2-mediated protein phosphorylation^{43,44,45}. Our data do not discount a similar post-transcriptional mechanism in *C. richardii*, or subtle guard cell gene expression changes may not have been detected by our whole-frond analysis. Although a previous mutant study of individual SnRK2 and SLAC genes in *C. richardii* failed to identify a role in stomatal closure²² our transcriptome assembly identified further SnRK2 and SLAC homologs (**Table S2**), raising the possibility of functional redundancy. Further *in vivo* testing is required to resolve whether the SnRK2-SLAC pathway functions in *C. richardii* stomatal closure. Conversely, homologs of genes involved in *Arabidopsis* downstream guard cell closure mechanisms (calcium and ROS signalling components, aquaporins and K⁺ ion channels)² were upregulated in association with *C. richardii* stomatal closure. The rapid nature of stomatal closure mechanisms in models such as *Arabidopsis* was thought to preclude the use of transcriptional regulation, but examples of stomatal movement depending on transcriptional activation have been reported^{46,47}. *C. richardii* stomatal responses appeared considerably slower than those of *Arabidopsis*, which might reflect a greater dependence on transcriptional regulation. Our results suggest that downstream components of active stomatal closure mechanisms are at least partially conserved between flowering plants and ferns.

21

22 **Stomatal sensitisation in *C. richardii* shares features with stomatal acclimation in flowering** 23 **plants**

Both dry and ABA pretreatment can condition stomatal sensitivity in *C. richardii*, inducing similar genome-wide changes in transcript abundance that enable active closure when subsequently exposed to low humidity. The stomata of flowering plants can also be sensitised or de-sensitised to closure-inducing signals through the process of acclimation. For example, newly-developed *Arabidopsis* stomata become increasingly sensitive to closure-promoting stimuli during leaf maturation in an ABA-dependent manner⁴⁸ whereas species transferred to high humidity conditions show impaired stomatal

1 closure when returned to lower humidity, despite accumulating ABA^{49,50}. In flowering plants, the
2 mechanism underlying altered guard cell sensitivity to ABA is thought to involve altered abundance of
3 the ABA receptors PYL/PYR/RCAR³⁴. Although there was no evidence of increased ABA receptor
4 abundance in sensitised *C. richardii* fronds, it is possible that the whole-frond dataset was not
5 sufficiently sensitive to detect all guard cell-specific changes. Sensitised fronds did exhibit reduced
6 abundance of an AtGRDP1 homolog²⁹, which negatively regulates expression of the ABA response
7 regulators *ABI3*⁵¹ and *ABI5*⁵², and whose loss of function leads to ABA hypersensitivity²⁹. Stomatal
8 sensitisation in *C. richardii* may therefore be related to increased sensitivity to ABA. As such,
9 conditional stomatal sensitivity in ferns and stomatal acclimation in flowering plants may both act by
10 altering the threshold at which subsequent inductive signals, including ABA, can trigger stomatal
11 closure.

12
13 Consistent with this idea, 24 closure-associated transcripts reduced in abundance during sensitisation,
14 all of which return to pre-sensitisation levels upon stomatal closure. These include all sensitisation
15 signature transcripts with calcium-binding and ROS-related annotations (**Data S2A** and **S3C**), plus
16 homologs of AtGRDP1 and AtPDR12, a guard cell ABA transporter²⁷. Although the transcript identified
17 was not directly orthologous to AtPDR12, more distantly-related *Arabidopsis* ABCG gene family
18 members also transport ABA (**Figure S2**)⁵³. We speculate that during sensitisation Ca²⁺, ROS and/or
19 ABA signalling cascades within the fern guard cell are potentiated to reduce the threshold required to
20 trigger them. Conversely, an ortholog of AtMRP4, which negatively regulates stomatal opening via
21 ABA-independent mechanisms²⁸, is up-regulated during sensitisation. AtPDR12 and AtMRP4 are both
22 strongly guard cell-expressed^{27,28}, whereas AtGRDP1 expression patterns have not been resolved²⁹.
23 The cell-type expression patterns of putative fern stomatal regulators identified here will need to be
24 confirmed experimentally in future studies. Eight sensitisation signature genes lack homologs in
25 *Arabidopsis* but have homologs in *P. patens* or *M. polymorpha*. Liverworts lack stomata, but only one
26 fern transcript had homology solely with this species. Fern stomatal regulatory networks may therefore
27 include elements lost in flowering plants but conserved with bryophyte signalling mechanisms.
28 Collectively, our results support a scenario whereby fern stomata are sensitised by altering the

intracellular physiological status of guard cells, enhancing their ability to respond to canonical closure signals and attenuating competing opening responses.

ACKNOWLEDGEMENTS

This work was supported by an ERC Advanced Investigator Grant (EDIP) to J.A.L., by a grant from the Gatsby Charitable Foundation to A.R.G.P. and A.M.H., and by Royal Society University Research Fellowships to A.R.G.P. and S.K. S.K. and D.E. were supported by the European Union's Horizon 2020 research and innovation programme under grant agreement number 637765. A.M.H. would like to acknowledge support from the Leverhulme Trust, RPG-2019-004 and the New Phytologist Foundation. We are grateful to Julie Bull and Ester Rabbino-witsch for support with plant watering, Prof. Julian Hibberd for providing growth space for RNA-seq experiments and to Pawel Baxter for performing NGS sequencing runs.

AUTHOR CONTRIBUTIONS

A.R.G.P. performed stomatal response assays, RNA extraction and next-generation sequencing library preparation. D.M.E. performed transcriptome assembly and bioinformatic analysis. A.R.G.P., A.M.H., J.A.L. and S.K. designed experiments. All authors contributed to preparation of the manuscript.

DECLARATION OF INTERESTS

The authors declare no competing interests.

FIGURE LEGENDS

Figure 1. Active closure of *C. richardii* stomata in response to low humidity and ABA is conditional on pre-exposure to either stimulus.

(**A-D**) Stomatal aperture areas from fronds of wet-grown ('Wet') versus dry-pretreated ('Dry') plants (**A** and **B**) or wet-grown plants pretreated with mock ('Mock') versus 100 μ M exogenous ABA solution ('ABA') (**C** and **D**), exposed to a low humidity stimulus (**A** and **C**) or maintained at high humidity (**B** and **D**) for 0, 60 or 120 minutes (as shown). Mock solution ('Mock') or 100 μ M ABA treatment ('ABA') was applied in an orthogonal design at the start of the assay. $N = 180$ stomata per pretreatment + treatment

combination (see STAR methods). Boxplots represent the 25th-75th percentile (box), median value (mid-line) further datapoints within 1.5x of the interquartile distance (whiskers). Pairwise comparisons were performed using two-tailed Mann-Whitney tests because stomatal aperture data did not meet the assumptions of ANOVA (see STAR Methods). Some comparisons required square root-transformation (**A**, **C** and **D**). Letters denote statistically significant differences ($p < 0.05$) within each plot. Pretreatment + treatment combinations with the same letter are not significantly different from each other. See also **Figure S1** and **Data S1A-E**.

Figure 2. *De novo* transcriptome assembly provides a robust platform for the identification of stomatal sensitisation and closure signatures.

(**A**) The design of RNA-seq sampling followed stomatal response assays, capturing whole-frond transcriptomes at 0 or 60 minutes from selected pretreatment + treatment + humidity combinations (as shown). Corresponding stomatal apertures, sensitivity and closure responses are shown for each timepoint sampled. Scale bars = 25 μ m.

(**B**) BUSCO analysis of transcript completeness within the *C. richardii* *de novo* transcript population assembled from (**A**). Protein-coding transcripts (proteome) were compared against reference proteomes (see STAR Methods), and all *de novo* assembled *C. richardii* transcripts were compared against the published genome assembly²⁵. Asterisks denote datasets generated by this study.

(**C**) Conservation and homology between *C. richardii* protein-coding transcripts identified within the *de novo* assembly and the *Arabidopsis* annotated genome⁶⁵.

See also **Table S1**.

Figure 3. Shared transcriptomic responses in both dry-pretreated and ABA-pretreated *C. richardii* fronds reflect a common underlying sensitisation process.

(**A**) Upset plot comparing transcripts with significantly different abundances between wet-grown versus dry-pretreated fronds or wet-grown versus ABA-pretreated fronds at two levels of stringency ($p < 0.05$ and $p < 0.01$). Transcripts with significantly different abundance ($p < 0.05$) under both pretreatments were classified as 'stomatal sensitisation signature' transcripts.

(B) Venn comparison between the abundance responses for each transcript with significantly altered transcript abundance ($p < 0.05$) within each pretreatment in (A). The central value (grey) represents all remaining assembled transcripts with unchanged abundance ($p > 0.05$).

See also **Figure S2** and **Data S2A-C**.

Figure 4. Homologs of genes underlying stomatal closure in *Arabidopsis* are also associated with closure in *C. richardii*.

(A) Upset plot comparing transcripts that accumulated to significantly different levels ($p < 0.01$) in association with stomatal closure between four different closure datasets (as shown). Within each dataset, transcripts specific to stomatal closure were identified by comparing between paired assays in which stomata did and did not close (**Figure S3**). 877 transcripts are associated with closure in at least two datasets ('Stomatal closure-associated'), 141 of which are present in at least three datasets ('Stomatal closure signature').

(B) Venn comparison between closure-associated transcripts (bold) and all assembled transcripts with homology to *Arabidopsis* genes with ABA or stomata-related functions (see STAR methods).

(C) Venn comparison between ABA/stomata-annotated closure-associated transcripts (B) and all assembled transcripts homologous to *Arabidopsis* regulators of stomatal signalling pathways and final effectors of closure. The *Arabidopsis* genes used to determine homology for each gene family represented are shown.

Underlined numbers in brackets (B and C) denote closure signature transcripts. See also **Figure S3**, **Table S2** and **Data S3A-B**.

Figure 5. Transcriptome profiles during stomatal closure and sensitisation suggest shared but opposing regulatory mechanisms that are largely ABA-independent.

(A) Upset plot comparing stomatal closure signature transcripts, all ABA and stomata-annotated transcripts and all transcripts with significantly altered abundance ($p < 0.01$) under ABA treatment at low or high humidity (as shown).

(B) Venn comparison between stomatal closure-associated transcripts (bold) and stomatal sensitisation signature transcripts.

(C) Venn comparison of the abundance changes between stomatal closure-associated transcripts during stomatal closure (bold) and sensitisation signature transcripts during stomatal sensitisation. The central value (grey) represents all remaining assembled transcripts with unchanged abundance ($p > 0.05$).

(D) Venn comparison between stomatal sensitisation signature transcripts, closure-associated transcripts and transcripts with significantly altered abundance ($p < 0.05$) between wet-grown fronds at high humidity (insensitive open stomata) and dry-pretreated fronds after 60 minutes low humidity (sensitised closing stomata).

Underlined numbers given in brackets (**B**, **C** and **D**) denote stomatal closure signature transcripts. See also **Figure S4**, **Data S3C** and **S4A-C**.

STAR METHODS

RESOURCE AVAILABILITY

Lead Contact

Requests for further information and resources generated by this study should be directed to and will be fulfilled by the Lead Contact, Andrew Plackett (A.R.G.Plackett@bham.ac.uk).

Materials Availability

This study did not generate any new unique reagents or materials.

Data and Code Availability

- RNA-seq data has been deposited at the NCBI Sequence Read Archive (raw sequence reads) and the NCBI Transcriptome Shotgun Assembly Sequence Database (assembled transcripts) and are publicly available as of the date of publication. Accession numbers are listed in the Key Resources Table. Protein sequences predicted from assembled transcripts have been deposited at Figshare and are publicly available as of the date of publication. DOIs are listed in the Key Resources Table. All individual stomatal measurements are provided in **Data S1B-1E**.
- This paper does not report any original code.

- Any additional information required to reanalyze the data reported in this paper is available from the lead contact upon request.

EXPERIMENTAL MODEL AND SUBJECT DETAILS

Plant material and growth conditions

Ceratopteris richardii wild-type laboratory strain Hn-n was used for all experiments⁵⁴. Gametophyte and sporophyte phases were grown under sterile culture on 'C-fern' solid growth media⁵⁵ (1% agar, pH 6.0) under 16 hour light/ 8 hour dark photoperiod at a fluence of 150 $\mu\text{mol m}^{-2} \text{s}^{-2}$ and constant 28°C temperature using a Fitotron SGC 120 plant growth chamber (Weiss Gallenkamp Ltd., Loughborough, UK). Spores were sterilized by incubation for 15 minutes in a $1/5$ dilution of sodium hypochlorite solution (Fisher Scientific, Loughborough, UK) plus 0.1% Tween20 detergent (Fisher Scientific, Loughborough, UK), followed by repeated rinsing in sterile water. After four days incubation in darkness at room temperature spores were sown onto 90 mm C-fern agar plates to germinate. Synchronised populations of sporophytes were generated by withholding water from gametophyte plates seven days after spore germination, and then flooding with sterile water at sexual maturity (11 days after germination) to allow free mating⁵⁶. Individual sporophytes were subsequently transferred to GA-7 Magenta boxes (Merck Life Science UK Ltd., Dorset, UK) containing 100 ml C-fern agar media when two fronds were visible (10-14 days old). Humidity was maintained by the application of 2 ml sterile water at the time of transplant, and subsequently when no surface water was visible (approximately every 14 days), with the time each box was opened to admit water minimised to maintain high humidity.

METHOD DETAILS

Stomatal pretreatment

Sporophytes were grown to 46-50 days old before sampling fronds for both stomatal response assays and RNA-seq. Plants were pretreated with either periodic low humidity or exogenous ABA application for a period of three weeks after transplant, then grown without further pretreatment for two weeks. During pretreatment, humidity conditions within magenta boxes were measured across three replicates using a TinyTag Plus2 data logger (Gemini Data Loggers, Chichester, UK). A constant high humidity of $94.9 \pm 0.36\%$ (\pm S.E.) was recorded within unopened Magenta boxes. 'Dry' pretreatment was applied

1 on alternating days three times a week by opening Magenta boxes to ambient humidity ($48.3 \pm 0.69\%$)
2 under sterile conditions for 10 minutes, during which time humidity within the boxes fell to $78.8 \pm 2.11\%$.
3 After boxes were closed internal humidity returned to $\geq 90\%$ in 3.3 ± 0.33 minutes. Plants under stable
4 high humidity ('wet-grown') pretreatment were incubated alongside dry-pretreated magenta boxes
5 during their exposure but were kept closed. ABA and mock pretreatments were delivered to plants
6 inside magenta boxes as $100 \mu\text{M}$ exogenous ABA in buffered solvent ($10 \text{ mM MES/KOH pH } 6.2$, 0.5%
7 Tween20 (v/v)) or a corresponding mock solution (0.1% EtOH in buffered solvent) respectively, applied
8 dropwise via Pasteur pipette (approximately $125 \mu\text{l}$) twice a week with the time each box was open
9 minimised to maintain high humidity. Opening magenta boxes for exogenous treatment or water
10 application caused a transient fall in recorded humidity to a minimum of $86.4 \pm 0.93\%$ at 7.0 ± 0.58
11 minutes after treatment, recovering to $\geq 90\%$ humidity after 22.7 ± 2.33 minutes.

12

13 **Stomatal response assay**

14 The responses of stomata from humidity- and ABA-pretreated plants were tested in separate assays.
15 Plants undergoing stomata response assays were also treated with $100 \mu\text{M}$ ABA or mock solution
16 (formulation as pretreatment) at the start of the assay (0 minutes), applied via an aerosol foliar spray
17 to maximise immediate surface contact and uptake. Treatments were applied orthogonally to humidity
18 or ABA pretreatments such that each pretreatment+treatment combination was represented by three
19 plants per assay. These three plants were each randomly assigned to a timepoint (0, 60 and 120
20 minutes from the assay start). Plants were either exposed to low humidity at 0 minutes by removal from
21 Magenta boxes into ambient air ($48.3 \pm 0.69\%$), or in control experiments maintained at high humidity
22 by immediately resealing Magenta boxes after ABA or mock treatment. At each timepoint a single frond
23 was sampled from one independent plant for each pretreatment+treatment combination and
24 photographed to record stomata morphology, selecting mature fronds from a similar shoot position on
25 each plant (frond 7-9, bearing 3 lobes). Three independent replicates were performed for each assay.
26 Stomata morphology was recorded by imaging under bright field microscopy at $10\times$ magnification using
27 an Olympus BX51 microscope (Olympus Corporation, Hamburg, Germany) with attached Qimaging
28 MP3.3-RTV-R-CLR-10-C MicroPublisher camera and QCapture Pro 7 software package (Teledyne
29 Photometrics, Tuscon, USA). Photography at each timepoint was completed within 15 minutes, and

pretreatment+treatment combinations were imaged in the same order between timepoints. Three separate regions were photographed on each frond (one within each lobe), selecting precise locations at random. Stomatal measurements were made from scaled images using the Fiji software package⁵⁷. Sixty stomata were measured per plant per pretreatment+treatment+timepoint combination, systematically selecting 20 stomata for measurement from each scaled photograph. All individual stomatal measurements and population-level summaries are provided in **Data S1A-E**. Whole-plant photography was performed using a Cybershot DSC-HX7V digital camera (Sony, Tokyo, Japan). During figure preparation images were adjusted for brightness and contrast using Photoshop 2019 (Adobe, San Jose, USA).

RNA extraction and sequencing

The sampling of frond tissue for RNA-seq was performed by snap-freezing single fronds in liquid nitrogen from specific pretreatment+treatment combinations at 0 or 60 minutes (**Figure 2A**). Three biological replicates were harvested for each pretreatment+treatment+timepoint combination, taken from three independently-performed assays. Harvesting of fronds at 0 minutes was conducted five hours after dawn (ZT5) for each assay. RNA was extracted using the RNeasy Plant mini kit with on-column DNase treatment (QIAGEN, Hilden, Germany). RNA quality was validated by Agilent 2100 Bioanalyzer RNA 6000 Pico assay (Agilent, Santa Clara, USA). Libraries were prepared from single frond samples using 1 µg starting RNA using the TruSeq RNA library prep kit V2 (Illumina Systems, San Diego, USA) and quantified by KAPA library quantification (Roche, Basel, Switzerland) on a CFX96 qPCR machine (Bio-Rad, Hercules, USA). Paired-end sequencing was performed by HiSeq2000 sequencing system using a NextSeq 500/550 High Output kit (150 cycles) (Illumina Systems, San Diego, USA).

Transcriptome assembly and annotation

Paired end reads were processed using rCorrector⁵⁸ with default parameters to correct likely erroneous k-mers. The Harvard FAS Informatics “FilterUncorrectablePEfastq” script (<https://github.com/harvardinformatics/TranscriptomeAssemblyTools>, accessed 13 January 2020) was used to discard read pairs for which one of the reads was deemed unfixable. TrimGalore

1 (https://www.bioinformatics.babraham.ac.uk/projects/trim_galore) was used with default settings to
2 trim adapter sequences and low-quality bases identified using the tools Cutadapt⁵⁹ and FastQC⁶⁰.
3 Reads were mapped to the SILVA rRNA SSUParc and LSUParc databases, release 132⁶¹ using Bowtie
4 2⁶² with option “--very-sensitive-local” and those pairs for which neither read was mapped to the rRNA
5 database were retained. Analysis using FastQC showed that the retained reads had per base
6 sequence content deviations greater the 5% from the mean for the first 7 and last 3 bases of the reads
7 and so these were clipped using TrimGalore. The transcriptome was assembled using Trinity⁶³ with
8 default settings.

9
10 A proteome was constructed by analysing the transcriptome using Transdecoder
11 (<http://transdecoder.sf.net>) “LongOrfs” and “Predict” with the Trinity gene-to-transcript map supplied as
12 input and with default parameters. Amino acid sequences were additionally identified for sequences
13 that were expressed above the minimum threshold for the differential expression analysis (> 1 CPM in
14 at least two biological replicates) but which had not yet had an amino acid sequence identified. This
15 was achieved using “TransDecoder.LongOrfs” with option “-m 10” to set a minimum length of 10 amino
16 acids. Those transcript sequences that did not return an open reading frame using TransDecoder were
17 subject to open reading frame prediction using GeneMark-ES⁶⁴.

18
19 To aid in the annotation of the differentially expressed transcripts, longest transcript variant proteomes
20 for the 12 species: *Arabidopsis thaliana* (TAIR10)⁶⁵, *Amborella trichopoda* (v1.0)⁶⁶, *Glycine max*
21 (Wm82.a4.v1)⁶⁷, *Manihot esculenta* (v7.1)⁶⁸, *Micromonas pusilla* CCMP1545 (v3.0)⁶⁹, *Ostreococcus*
22 *lucimarinus* (v2.0)⁷⁰, *Oryza sativa* (v7.0)⁷¹, *Physcomitrium patens* (v3.3)⁷², *Solanum lycopersicum*
23 (ITAG3.2)⁷³, *Selaginella moellendorffii* (v1.0)⁷⁴, *Spirodela polyrhiza* (v2)⁷⁵ and *Volvox carteri* (v2.1)⁷⁶
24 were downloaded from Phytozome⁷⁷. OrthoFinder 2.3.11⁷⁸ was used with default settings to assign the
25 genes to orthogroups and to identifying orthologs for the *C. richardii* proteome. GO^{79,80}, Plant
26 Ontology⁸¹ and MapMan⁸² annotations for *Arabidopsis* were downloaded from The Arabidopsis
27 Information Resource (TAIR)⁶⁵. Each orthogroup inherited the annotations of the *Arabidopsis* genes
28 that it contained. The same reference proteomes were compared against the predicted *C. richardii*

proteome by BUSCO analysis⁸³ using the viridiplantae_odb10 dataset to assess their relative completeness.

To identify homologs of the annotated protein coding genes a series of searches were carried out, terminating at the first success for each gene. These searches were for: an ortholog in *Arabidopsis* identified by OrthoFinder, an *Arabidopsis* homolog from within the same OrthoFinder orthogroup, any significant DIAMOND⁸⁴ hit to an *Arabidopsis* homolog ($e < 10^{-3}$), any significant hit for a homolog within the 12 plant species above, any significant hit within the BLAST nr database⁸⁵. An additional OrthoFinder analysis was performed with the addition of *M. polymorpha* to the previous analysis to identify orthologs and homologs in that species. The *M. polymorpha* proteome (v3.1)⁸⁶ was downloaded from Phytozome⁷⁷. Gene homologs for each individual transcript are provided together with pairwise comparison expression data between frond samples given in **Data S2B-C, S3D-J and S4D-E**. If OrthoFinder determined that there was not an *Arabidopsis* ortholog, then the closest homolog is listed preceded by a "~". Where no homologs were identified within these species, the closest sequence identified within the BLAST nr database is given if a significant hit was found.

Phylogenetic analysis

Sequences included in phylogenetic analyses were selected based upon target orthogroups generated during transcriptome annotation, excluding *Glycine max* and *Manihot esculenta* to allow clearer presentation. Sequences were aligned using MAFFT L-INS-I and maximum-likelihood trees were inferred using IQ-TREE⁸⁷ with options -m TEST -bb 1000 (best model test and 1000 bootstrap replicates). Graphical representations were generated using iTOL v6 (<https://itol.embl.de/>)⁸⁸ and annotated using Photoshop 2019.

QUANTIFICATION AND STATISTICAL ANALYSIS

Stomatal response quantification

Statistical analysis of stomatal measurements was performed in R (version 3.6.3)⁸⁹ using the car software package⁹⁰. Dataset distributions were tested for Normality using the Shapiro-Wilk test⁹¹, which determined that the assumptions of ANOVA and pairwise T tests could not be adequately met across

all comparisons between pretreatment+treatment combinations. Comparisons were tested for equal variance using Levene's test⁹². Pairwise comparisons were instead performed using two-tailed Mann-Whitney tests, with post-hoc adjustment of p-values for multiple comparisons (Benjamini-Hochberg procedure)⁹³. Details of dataset size (n = number of stomata), significance threshold, dispersion parameters and data transformations needed to meet the assumptions of the Mann-Whitney test are provided in the legends of **Figure 1** and **Figure S1**. Boxplots were prepared using the ggplot2 software package using default settings⁹⁴.

Transcript abundance analysis

Transcript abundance estimation was performed using Salmon⁹⁵ within the Trinity pipeline. Differential expression testing was performed using DESeq2⁹⁶ (options "-min_reps_min_cpm 2,1") also with the Trinity pipeline. Abundance of individual transcripts was compared between three biological replicates of each sample ($n = 3$). All differential expression comparisons between sample pairs are given in **Data S2B-C, S3D-J** and **S4D-E**. The significance threshold used for each comparison is provided in **Figures 3, 4** and **5** and **Figures S2, S3** and **S4**. Venn diagrams were generated using the InteractiVenn web tool⁹⁷. Upset plots were generated in R using the UpSetR software package⁹⁸.

SUPPLEMENTAL INFORMATION

Data S1. *C. richardii* stomatal response assay measurements in response to low or high humidity, Related to Figure 1.

(A) *C. richardii* stomatal area summary statistics under each pretreatment+treatment+timepoint.

(B-E) Individual stomatal measurements from wet-grown versus dry-pretreated plants (B and C) and mock-pretreated versus ABA-pretreated plants (D and E) from stomatal response assays under low humidity (B and D) and high humidity conditions (C and E).

Data S2. Additional annotation and homology of *C. richardii* stomatal sensitisation signature transcripts, Related to Figure 3.

(A) Stomatal sensitisation signature transcript IDs, expression responses to pretreatment, homology to other species and assigned functional annotations.

(**B** and **C**) Pairwise comparison of the abundance of individual transcripts in fronds at timepoint 0 between wet-grown versus dry-pretreated plants (**B**) and wet-grown versus dry-pretreated plants (**C**).

Data S3. Additional annotation and homology of *C. richardii* stomatal closure-associated transcripts, Related to Figures 4 and 5.

(**A**) Identities of individual stomatal closure-associated and closure signature transcripts (**Figure 4A**), obtained through comparison of closure candidate transcripts between multiple closure assays (**Figure S3A-D**).

(**B**) Identities of individual stomatal closure-associated and closure signature transcripts homologous to *Arabidopsis* genes with annotations relating to ABA or stomata (**Figure 4B** and **C**).

(**C**) Identities of individual transcripts common to both stomatal closure-associated and stomatal sensitisation signature datasets (**Figure 5B**).

(**D-J**) Pairwise comparisons of the abundance of individual transcripts in fronds from wet-grown plants between 0 minutes versus 60 minutes low humidity + mock treatment (no stomatal response) (**D**), fronds from dry-pretreated plants between 0 minutes versus 60 minutes low humidity + mock treatment (stomatal closure induced) (**E**), fronds from dry-pretreated plants between 0 minutes versus 60 minutes high humidity + mock treatment (no stomatal response) (**F**), fronds from dry-pretreated plants between 0 minutes versus 60 minutes low humidity + ABA treatment (enhanced stomatal closure) (**G**), fronds from dry-pretreated plants between 0 minutes versus 60 minutes high humidity + ABA treatment (no stomatal response) (**H**), fronds from ABA-pretreated plants between 0 minutes versus 60 minutes low humidity + mock treatment (stomatal closure induced) (**I**) and between wet-grown plants at 0 minutes versus fronds from dry-pretreated plants after 60 minutes low humidity (stomata sensitised and closure induced) (**J**).

Data S4. *C. richardii* transcripts responsive to ABA under either low or high humidity, Related to Figure 5.

(**A**) Identities of all individual transcripts demonstrating a significant change in abundance ($p < 0.01$) in response to ABA treatment under low humidity and/or high humidity (**Figure 5A** and **Figure S4A-C**).

(B) Identities of individual stomatal closure-associated and stomatal sensitisation signature transcripts that demonstrate a significant change in abundance in response to ABA treatment ($p < 0.01$) under low humidity and/or high humidity (**Figure 5A** and **Figure S4D**).

(C) Identities of individual transcripts with homology of stomata-annotated *Arabidopsis* genes that demonstrate a significant change in abundance in response to ABA treatment ($p < 0.01$) under low humidity and/or high humidity (**Figure 5A** and **Figure S4E**).

(D and E) Pairwise comparisons of the abundance of individual transcripts in fronds from dry-pretreated plants between 60 minutes mock versus 60 minutes ABA treatment at low humidity (D) and between 60 minutes mock versus 60 minutes ABA treatment at high humidity (E).

REFERENCES

1. Raven, J.A. (2008). Selection pressures on stomatal evolution. *New Phytol.* 153, 371-386. 10.1046/j.0028-646X.2001.00334.x.
2. Munemasa, S., Hauser, F., Park, J., Waadt, R., Brandt, B., and Schroeder, J.I. (2015). Mechanisms of abscisic acid-mediated control of stomata aperture. *Curr. Op. Plant Biol.* 28, 154-162. 10.1016/j.pbi.2015.10.010.
3. Assmann, S.M., and Jegla, T. (2016). Guard cell sensory systems, recent insights on stomatal responses to light, abscisic acid, and CO₂. *Curr. Opin. Plant Biol.* 33, 157-167. 10.1016/j.pbi.2016.07.003.
4. Lawson T., and Matthews, J. (2020). Guard cell metabolism and stomata function. *Ann. Rev. Plant Biol.* 71, 273-302. 10.1146/annurev-arplant-050718-100251.
5. Kenrick, P., and Crane, P.R. (1997). The origin and early diversification of land plants. A cladistic study. (Smithsonian Institution Press).
6. Harris, B.J., Harrison, C.J., Hetherington, A.M., and Williams, T.A. (2020). Phylogenomic evidence for the monophyly of bryophytes and the reductive evolution of stomata. *Curr. Biol.* 30, 2001-2012. 10.1016/j.cub.2020.03.048.
7. Chater, C., Kamisugi, Y., Movahedi, M., Fleming, A., Cuming, A.C., Gray, J.E., and Beerling, D.J. (2011). Regulatory mechanism controlling stomatal behavior conserved across 400 million years of land plant evolution. *Curr. Biol.* 21, 1025-1029. 10.1016/j.cub.2011.04.032.

1 8. Lind, C., Dreyer, I., López-Sanjurjo, E.J., von Meyer, K., Ishizaki, K., Kohchi, T., Lang, D., Zhao, Y.,
2 Kreuser, I., Al-Rasheid, K.A.S. *et al.* (2015). Stomatal guard cells co-opted an ancient ABA-dependent
3 desiccation survival system to regulate stomatal closure. *Curr. Biol.* 25, 928-935.
4 10.1016/j.cub.2015.01.067.

5 9. Cai, S., Chen, G., Wang, Y., Huang, Y., Marchant, D.B., Wang, Y., Yang, Q., Dai, F., Hills, A., Franks,
6 P.J. *et al.* (2017). Evolutionary conservation of ABA signalling for stomatal closure. *Plant Physiol.* 174,
7 732-747. 10.1104/pp.16.01848.

8 10. Pressel, S., Renzaglia, K.S., Clymo, R.S., and Duckett, J.G. (2018). Hornwort stomata do not
9 respond actively to exogenous and environmental cues. *Ann. Bot.* 122, 45-57. 10.1093/aob/mcy045.

10 11. Brodribb, T.J., and McAdam, S.A.M. (2011). Passive origins of stomatal control in vascular plants.
11 *Science* 331, 582-585. 10.1126/science.1197985.

12 12. McAdam, S.A.M., and Brodribb, T.J. (2012). Fern and lycopphyte guard cells do not respond to
13 endogenous abscisic acid. *Plant Cell* 24, 1510-1521. 10.1105/tpc.112.096404.

14 13. McAdam, S.A.M., and Brodribb, T.J. (2013). Ancestral stomatal control results in a canalization of
15 fern and lycopphyte adaptation to drought. *New Phytol.* 198, 429-441. 10.1111/nph.12190.

16 14. Martins, S.C.V., McAdam, S.A.M., Deans, R.M., DaMatta, F.M., and Brodribb, T.J. (2016). Stomatal
17 dynamics are limited by leaf hydraulics in ferns and conifers: results from simultaneous measurements
18 of liquid and vapour fluxes in leaves. *Plant Cell Environ.* 39, 694-705. 10.1111/pce.12668.

19 15. Cardoso, A.A., Randall, J.M., and McAdam, S.A.M. (2019). Hydraulics regulate stomatal responses
20 to changes in leaf water status in the fern *Athyrium felix-femina*. *Plant Physiol.* 179, 533-543.
21 10.1104/pp.18.01412.

22 16. Ruszala, E.M., Beerling, D.J., Franks, P.J., Chater, C., Casson, S.A., Gray, J.E., and Hetherington,
23 A.M. (2011). Land plants acquired active stomatal control early in their evolutionary history. *Curr. Biol.*
24 21, 1030-1035. 10.1016/j.cub.2011.04.044.

25 17. Franks, P.J., Britton-Harper, Z.J. (2016). No evidence of general CO₂ insensitivity in ferns: one
26 stomatal control mechanism for all land plants? *New Phytol.* 211, 819-827. 10.1111/nph.14020.

27 18. Horak, H., Kollist, H., and Merilo, E. (2017). Fern stomatal responses to ABA and CO₂ depend on
28 species and growth conditions. *Plant Physiol.* 174, 672-679. 10.1104/pp.17.00120.

1 19. Grantz, D.A., Linscheid, B.S., and Grulke, N.E. (2019). Differential responses of stomatal kinetics
2 and steady-state conductance to abscisic acid in a fern: comparison with a gymnosperm and an
3 angiosperm. *New Phytol.* 222, 1883-1892. 10.1111/nph.15736.

4 20. Kübarsepp, L., Laanisto, L., Niinemets, Ü., Talts, E., and Tosens, T. (2020). Are stomata in ferns
5 and allies sluggish? Stomatal responses to CO₂, humidity and light and their scaling with size and
6 density. *New Phytol.* 225, 183-195. 10.1111/nph.16159.

7 21. Wu, T.C., Lin, B.L., and Kao, W.Y. (2020). Active stomatal control of *Marsilea crenata*, an
8 amphibious fern, in response to CO₂ and exogenous application of ABA. *Taiwania* 65, 431-437.
9 10.6165/tai.2020.65.431.

10 22. McAdam, S.A.M., Brodribb, T.J., Banks, J.A., Hedrich, R., Atallah, N.M., Cai, C., Geringer, M.A.,
11 Lind, C., Nichols, D.S., Stachowski, K. *et al.* (2016). Absciscic acid controlled sex before transpiration
12 in vascular plants. *Proc. Nat. Acad. Sci. USA* 113, 12862-12867. 10.1073/pnas.1606614113.

13 23. Banks, J.A. (1994). Sex-determining genes in the homosporous fern *Ceratopteris*. *Dev.* 120, 1949-
14 1958.

15 24. Hickok, L.G., Warne, T.R., and Fribourg, R.S. (1995). The biology of the fern *Ceratopteris* and its
16 use as a model system. *Int. J. Plant Sci.* 156, 332-345. 10.1086/297255.

17 25. Marchant, D.B., Sessa, E.B., Wolf, P.G., Heo, K., Barbuzak, W.B., Soltis, P.S., and Soltis, D.E.
18 (2019). The C-Fern (*Ceratopteris richardii*) genome: insights into plant genome evolution with the first
19 partial homosporous fern genome assembly. *Nat. Sci. Rep.* 9, 18181. 10.1038/s41598-019-53968.

20 26. Geng, Y., Cai, C., McAdam, S.A.M., Banks, J.A., Wisecaver, J.H., and Zhou, Y. (2021). A de novo
21 transcriptome assembly of *Ceratopteris richardii* provides insights into the evolutionary dynamics of
22 complex gene families in land plants. *Genome Biol. Evol.* 13, evab042. 10.1093/gbe/evab042.

23 27. Kang, J., Hwang, J.U., Lee, M., Kim, Y.Y., Assman, S.M., Martinoia, E., and Lee, Y. (2010). PDR-
24 type ABC transporter mediates cellular uptake of the phytohormone abscisic acid. *Proc. Nat. Acad.*
25 *Sci. USA* 107, 2355-2360. 10.1073/pnas.0909222107.

26 28. Klein, M., Geisler, M., Suh, S.J., Kolukisaoglu, H.Ü., Azevedo, L., Plaza, S., Curtis, M.D., Richter,
27 A., Weder, B., Schulz, B. *et al.* (2004). Disruption of *AtMPR4*, a guard cell plasma membrane ABCC-
28 type ABC transporter, leads to deregulation of stomatal opening and increased drought susceptibility.
29 *Plant J.* 39, 219-236. 10.1111/j.1365-313X.2004.02125.x.

29. Rodríguez-Hernández, A.A., Ortega-Amaro, M.A., Delgado-Sánchez, P., Salinas, J., and Jiménez-Bremont, J.F. (2014). *AtGRDP1* gene encoding a glycine-rich domain protein is involved in germination and responds to ABA signalling. *Plant Mol. Biol. Rep.* 32, 1187-1202. 10.1007/s11105-014-0714-4.

30. Singh, D., and Laxmi, A. (2015). Transcriptional regulation of drought response: a torturous network of transcription factors. *Front. Plant Sci.* 6, 895. 10.3389/fpls.2015.00895.

31. Mittler, R., and Blumwald, E. (2015). The roles of ROS and ABA in systemic-acquired acclimation. *Plant Cell* 27, 64-70. 10.1105/tpc.114.133090.

32. Véry, A.A., and Sentenac, H. (2002). Cation channels in the *Arabidopsis* plasma membrane. *Trends Plant Sci.* 7, 168-175. 10.1016/S1360-1385(02)02262-8.

33. Chater, C.C., Caine, R.S., Tomek, M., Wallace, S., Kamisugi, Y., Cuming A.C., Lang, D., MacAlister, C.A., Casson, S., Bergmann, D.C. *et al.* (2016). Origin and function of stomata in the moss *Physcomitrella patens*. *Nature Plants* 2, 16179. 10.1038/NPLANTS.2016.179.

34. Dittrich, M., Mueller, H.M., Bauer, H., Peirats-Llobet, M., Rodriguez, P.L., Geilfus, C.M., Carpentier, S.C., Al Rasheid, K.A.S., Kollist, H., Merilo, E. *et al.* (2019). The role of *Arabidopsis* ABA receptors from the PYR/PYL/RCAR family in stomatal acclimation and closure signal integration. *Nat. Plants* 5, 1002-1011. 10.1038/s41477-019-0490-0.

35. Cai, S., Huang, Y., Chen, F., Zhang, X., Sessa, E.B., Zhao, C., Marchant, D.B., Xue, D., Chen, G., Dai, F. *et al.* (2021). Evolution of rapid blue-light response linked to explosive diversification of ferns in Angiosperm forests. *New Phytol.* 10.1111/nph.17135.

36. Inoue, S.I., and Kinoshita, T. (2017). Blue light regulation of stomatal opening and the plasma membrane H⁺-ATPase. *Plant Physiol.* 174, 531-538. 10.1104/pp.17.00166.

37. Ma, Y., Szostkiewicz, I., Korte, A., Moes, D., Yang, Y., Christmann, A., and Grill, E. (2009). Regulators of PP2C phosphatase activity function as abscisic acid sensors. *Science* 324, 1064-1068. 10.1126/science.1172408.

38. Park, S.Y., Fung, P., Nishimura, N., Jensen, D.R., Fujii, H., Zhao, Y., Lumba, S., Santiago, J., Rodrigues, A., Chow, T.F. *et al.* (2009). Absciscic acid inhibits type 2C protein phosphatases via the PYR/PYL family of START proteins. *Science* 324, 1068-1071. 10.1126/science.1173041.

39. Santiago, J., Rodrigues, A., Saez, A., Rubio, S., Antoni, R., Dupeux, F., Park, S.Y., Márquez, J.A., Cutler, S.R., and Rodriguez, P.L. (2009). Modulation of drought resistance by the abscisic acid receptor PYL5 through inhibition of clade A PP2Cs. *Plant J.* **60**, 575-588. 10.1111/j.1365-313X.2009.03981.x.
40. Mustilli, A.-C., Merlot, S., Vavasseur, A., Fenzi, F., and Giraudat, J. (2002). Arabidopsis OST1 protein kinase mediates the regulation of stomatal aperture by abscisic acid and acts upstream of reactive oxygen species production. *Plant Cell* **14**, 3089-3099. 10.1105/tpc.007906.
41. Negi, J., Matsuda, O., Nagasawa, T., Oba, Y., Takahashi, H., Kawai-Yamada, M., Uchimiya, H., Hashimoto, M., and Iba, K. (2008). CO₂ regulator SLAC1 and its homologues are essential for anion homeostasis in plant cells. *Nature* **452**, 483-486.
42. Vahisalu, T., Kollist, H., Wang, Y.F., Nishimura, N., Chan, W.Y., Valerio, G., Lamminmäki, A., Brosché, M., Moldau, H., Desikan, R. *et al.* (2008). SLAC1 is required for plant guard cell S-type anion channel function in stomatal signalling. *Nature* **452**, 487-491. 10.1038/nature0660.
43. Umezawa, T., Sugiyama, N., Mizoguchi, M., Hayashi, S., Myouga, F., Yamaguchi-Shinozaki, K., Ishihama, Y., Hirayama, T., and Shinozaki, K (2009). Type 2 protein phosphatases directly regulate abscisic acid-activated protein kinases in *Arabidopsis*. *Proc. Nat. Acad. Sci. USA* **106**, 17588-17593. 10.1073/pnas.0907095106.
44. Vlad, F., Rubio, S., Rodrigues, A., Sirichandra, C., Belin, C., Robert, N., Leung, J., Rodriguez, P.L., Laurière, C., and Merlot, S. (2009). Protein phosphatases 2C regulate the activation of Snf-1 Related Kinase OST1 by abscisic acid in *Arabidopsis*. *Plant Cell* **21**, 3170-3184. 10.1105/tpc.109.069179.
45. Brandt, B., Brodsky, D.E., Xue, S., Negi, J., Iba, K., Kangasjärvi, J., Ghassemien, M., Stephan, A.B., Hu, H., and Schroeder, J.I. (2012). Reconstitution of abscisic acid activation of SLAC1 anion channel by CPK6 and OST1 kinases and branched ABI1 PP2C phosphatase action. *Proc. Nat. Acad. Sci. USA* **109**, 10593-10598. 10.1073/pnas.1116590109.
46. Liang, Y.K., Dubos, C., Dodd, I.C., Holroyd, G.H., Hetherington, A.M., and Campbell, M.M. (2005). AtMYB61, and R2R3-MYB transcription factor controlling stomatal aperture in *Arabidopsis thaliana*. *Curr. Biol.* **15**, 1201-1206. 10.1016/j.cub.2005.06.041.
47. Cominelli, E., Galbiati, M., Vavasseur, A., Conti, L., Sala, T., Vuylsteke, M., Leonhardt, N., Dellaporta, S.L., and Tonelli, C. (2005). A guard-cell-specific MYB transcription factor regulates

1 stomatal movements and plant drought tolerance. *Curr. Biol.* 15, 1196-1200.
2 10.1016/j.cub.2005.05.048.

3 48. Pantin, F., Renaud, J., Barbier, F., Vavasseur, A., Le Thiec, D., Rose, C., Bariac, T., Casson, S.,
4 McLachlan, D.H., Hetherington, A.M. *et al.* (2013). Developmental priming of stomatal sensitivity to
5 abscisic acid by leaf microclimate. *Curr. Biol.* 23, 1805-1811. 10.1016/j.cub.2013.07.050.

6 49. Fordham, M.C., Harrison-Murray, R.S., Knight, L., and Evered, C.E. (2001). Effects of leaf wetting
7 and high humidity on stomatal function in leafy cuttings and intact plants of *Corylus maxima*.
8 *Physiologia plantarum* 113, 233-240. 10.1034/j.1399-3054.2001.1130211.x.

9 50. Rezaei Nejad, A., and van Meeteren, U. (2008). Dynamics of adaptation of stomatal behaviour to
10 moderate or high relative air humidity in *Tradescantia virginiana*. *J. Exp. Bot.* 59, 289-301.
11 10.1093/jxb/erm308.

12 51. Parcy, F., and Giraudat, J. (1997). Interactions between the *ABI1* and the ectopically expressed
13 *ABI3* genes in controlling abscisic acid responses in *Arabidopsis* vegetative tissues. *Plant J.* 11, 693-
14 702. 10.1046/j.1365-313X.1997.11040693.x

15 52. Lopez-Molina, L., Mongrand, S., and Chua, N.H. (2001). A postgermination developmental arrest
16 checkpoint is mediated by abscisic acid and requires the ABI5 transcription factor in *Arabidopsis*. *Proc.*
17 *Nat. Acad. Sci. USA* 98, 4782-4787. 10.1073/pnas.081594298.

18 53. Gräfe, K., and Schmitt, L (2021). The ABC transporter G subfamily in *Arabidopsis thaliana*. *J. Exp.*
19 *Bot.* 72, 92-106. 10.1093/jxb/eraa260.

20 54. Warne, T.R., and Hickok, L.G. (1987). (2-Chloroethyl)phosphonic acid promotes germination of
21 immature spores of *Ceratopteris richardii* Brongn. *Plant Physiol.* 83, 723–725. 10.1104/pp.83.4.723.

22 55. Hickok, L.G., and Warne, T.R. (1998). C-Fern manual. Carolina Biological Supply Company,
23 Burlington, VT.

24 56. Plackett, A.R.G., Rabbinowitsch, E.H., and Langdale, J.A. (2015). Protocol: genetic transformation
25 of the fern *Ceratopteris richardii* through microparticle bombardment. *Plant Methods* 11, 37.
26 10.1186/s13007-015-0080-8.

27 57. Schindelin, J., Arganda-Carreras, I., Frise, E., Kaynig, V., Longair, M., Pietzsch, T., Preibisch, S.,
28 Rueden, C., Saalfeld, S., Schmid, B. *et al.* (2012). Fiji: an open-source platform for biological-image
29 analysis. *Nat. Methods* 9, 676-682. 10.1038/nmeth.2019.

58. Song, L., and Florea, L. (2015). Rcorrector: Efficient and accurate error correction for Illumina RNA-seq reads. *GigaScience* 4, 48. 10.1186/s13742-015-0089-y.

59. Martin, M. (2011). Cutadapt removes adapter sequences from high-throughput sequencing reads. *EMBnet.journal* 17, 10-12. 10.14806/ej.17.1.200.

60. Andrews, S. (2010). FastQC: A Quality Control Tool for High Throughput Sequence Data. <http://www.bioinformatics.babraham.ac.uk/projects/fastqc>.

61. Quast, C., Pruesse, E., Yilmaz, P., Gerken, J., Schweer, T., Yarza, P., Peplies, J., and Glöckner, F.O. (2013). The SILVA ribosomal RNA gene database project: improved data processing and web-based tools. *Nucl. Acids Res.* 41, D590-D596. 10.1093/nar/gks1219.

62. Langmead, B., and Salzberg, S. (2012). Fast gapped-read alignment with Bowtie 2. *Nature Methods* 9, 357-359. 10.1038/nmeth.1923.

63. Haas, B.J., Papanicolaou, A., Yassour, M., Grabherr, M., Blood, P.D., Bowden, J., Couger, M.B., Eccles, D., Li, B., Lieber, M. *et al.* (2013). *De novo* transcript sequence reconstruction from RNA-seq using the Trinity platform for reference generation and analysis. *Nat. Protoc.* 8, 1494–1512. 10.1038/nprot.2013.084.

64. Ter-Hovhannisyan, V., Lomsadze, A., Chernoff, Y., and Borodovsky, M. (2008). Gene prediction in novel fungal genomes using an ab initio algorithm with unsupervised training. *Genome Research* 18, 1979-1990. 10.1101/gr.081612.108.

65. Berardini, T.Z., Reiser, L., Li, D., Mezheritsky, Y., Muller, R., Strait, E., and Huala, E. (2015). The Arabidopsis Information Resource: Making and mining the "gold standard" annotated reference plant genome. *Genesis* 53, 474-485. 10.1002/dvg.22877.

66. Chamala, S., Chanderbali, A.S., Der, J.P., Lan, T., Walts, B., Albert, V.A., dePamphilis, C.W., Leebens-Mack, J., Rounsley, S., Schuster S.C. *et al.* (2013). Assembly and validation of the genome of the nonmodel basal angiosperm Amborella. *Science* 342, 1516-1517. 10.1126/science.1241130.

67. Schmutz, J., Cannon, S.B., Schlueter, J., Ma, J., Mitros, T., Nelson, W., Hyten, D.L., Song, Q., Thelan, J.J., Cheng, J. *et al.* (2010). Genome sequence of the palaeopolyploid soybean. *Nature* 463, 178-183. 10.1038/nature08670.

68. Bredeson, J.V., Lyons, J.B., Prochnik, S.E., Wu, G.A., Ha, C.M., Edsinger-Gonzales, E., Grimwood, J., Schmutz, J., Rabbi, I.Y., Egesi, C. *et al.* (2016). Sequencing wild and cultivated cassava and related

1 species reveals extensive interspecific hybridization and genetic diversity. *Nat. Biotechnol.* **34**, 562-
2 570. 10.1038/nbt.3535.

3 69. Worden, A.Z., Lee, J.H., Mock, T., Rouzé, P., Simmons, M.P., Aerts, A.L., Allen, A.E., Cuvelier,
4 M.L., Derelle, E., Everett M.V. *et al.* (2009). Green evolution and dynamic adaptations revealed by
5 genomes of the marine picoeukaryotes *Micromonas*. *Science* **324**, 268-272.
6 10.1126/science.1167222.

7 70. Palenik, B., Grimwood, J., Aerts, A., Rouzé, P., Salamov, A., Putnam, N., Dupont, C., Jorgensen,
8 R., Derelle, E., Rombauts, S. *et al.* (2007). The tiny eukaryote *Ostreococcus* provides genomic insights
9 into the paradox of plankton speciation. *Proc. Nat. Acad. Sci. USA* **104**, 7705-7710.
10 10.1073/pnas.0611046104.

11 71. Ouyang, S., Zhu, W., Hamilton, J., Lin, H., Campbell, M., Childs, K., Thibaud-Nissen, F., Malek,
12 R.L., Lee, Y., Zheng, L. *et al.* (2007). The TIGR Rice Genome Annotation Resource: improvements
13 and new features., *Nucleic Acids Res.* **35**, D883-D887. 10.1093/nar/gkl976.

14 72. Lang, D., Ullrich, K.K., Murat, F., Fuchs, J., Jenkins, J., Haas, F.B., Piednoel, M., Gundlach, H.,
15 Van Bel, M., Meyberg, R. *et al.* (2018). The *Physcomitrella patens* chromosome-scale assembly
16 reveals moss genome structure and evolution. *Plant J* **93**, 515-533. 10.1111/tpj.13801.

17 73. The Tomato Genome Consortium (2012). The tomato genome sequence provides insights into
18 fleshy fruit evolution. *Nature* **485**, 635-641. 10.1038/nature11119.

19 74. Banks, J.A., Nishiyama, T., Hasebe, M., Bowman, J.L., Gribskov, M., dePamphilis, C., Albert, V.A.,
20 Aono, N., Aoyama, T., Ambrose, B.A. *et al.* (2011). The *Selaginella* genome identifies genetic changes
21 associated with the evolution of vascular plants. *Science* **332**, 960-963. 10.1126/science.1203810.

22 75. Wang, W., Haberer, G., Gundlach, H., Gläßer, C., Nussbaumer, T., Luo, M.C., Lomsadze, A.,
23 Borodovsky, M., Kerstetter, R.A., Shanklin, J. *et al.* (2014). The *Spirodela polyrhiza* genome reveals
24 insights into its neotenuous reduction fast growth and aquatic lifestyle. *Nat. Commun.* **5**, 3311.
25 10.1038/ncomms4311.

26 76. Prochnik, S.E., Umen, J., Nedelcu, A.M., Hallmann, A., Miller, S.M., Nishii, I., Ferris, P., Kuo, A.,
27 Mitros, T., Fritz-Laylin, L.K. *et al.* (2010). Genomic analysis of organismal complexity in the multicellular
28 green alga *Volvox carteri*. *Science* **329**, 223-226. 10.1126/science.1188800.

1 77. Goodstein, D.M., Shu, S., Howson, R., Neupane, R., Hayes, R.D., Fazo, J., Mitros, T., Dirks, W.,
2 Hellsten, U., Putnam, N. *et al.* (2012). Phytozome: a comparative platform for green plant genomics.
3 Nucleic Acids Research *40*, D1178–D1186. 10.1093/nar/gkr944.

4 78. Emms, D.M., and Kelly, S. (2019). Orthofinder: phylogenetic orthology inference for comparative
5 genomics. Genome Biology *20*, 238. 10.1186/s13059-019-1832-y.

6 79. Ashburner, M., Ball, C.A., Blake, J.A., Botstein, D., Butler, H., Cherry, J.M., Davis, A.P., Dolinsky,
7 K., Dwight, S.S., Eppig, J.T. *et al.* (2000). Gene Ontology: tool for the unification of biology. Nat Genet.
8 *25*, 25-29. 10.1038/75556.

9 80. The Gene Ontology Consortium (2019). The Gene Ontology Resource: 20 years and still GOing
10 strong. Nucleic Acids Res. *47*, D330-D338. 10.1093/nar/gky1055.

11 81. Walls, R.L., Cooper, L., Elser, J., Gandolfo, M.A., Mungall, C.J., Smith, B., Stevenson, D.W., and
12 Jaiswal, P. (2019). The Plant Ontology Facilitates Comparisons of Plant Development Stages Across
13 Species. Front. Plant Sci. *10*, 631. 10.3389/fpls.2019.00631.

14 82. Thimm, O., Blaesing, O., Gibon, Y., Nagel, A., Meyer, S., Krüger, P., Selbig, J., Müller, L.A., Rhee,
15 S.Y., and Stitt, M. (2004). MAPMAN: a user-driven tool to display genomics data sets onto diagrams
16 of metabolic pathways and other biological processes. Plant J. *37*, 914-39. 10.1111/j.1365-
17 313X.2004.02016.x.

18 83. Simão, F.A., Waterhouse, R.M., Ioannidis, P., Kriventseva, E.V., and Zdobnov, E.M. (2015).
19 BUSCO: assessing genome assembly and annotation completeness with single-copy orthologs.
20 Bioinformatics *31*, 3210-3212. 10.1093/bioinformatics/btv351.

21 84. Buchfink, B., Xie, C., and Huson, D.H. (2015). Fast and sensitive protein alignment using
22 DIAMOND. Nat. Meth. *12*, 59. 10.1038/nmeth.3176.

23 85. NCBI Resource Co-ordinators (2016). Database resources of the National Center for Biotechnology
24 Information. Nuc. Acid Res. *44*, D7-D19. 10.1093/nar/gkv1290.

25 86. Bowman, J.L., Kohchi, T., Yamato, K.T., Jenkins, J., Shu, S., Ishizaki, K., Yamaoka, S.,
26 Nishihama, R., Nakamura, Y., Berger, F. *et al.* (2017). Insights into land plant evolution garnered
27 from the *Marchantia polymorpha* genome. Cell *171*, 287-304. 10.1016/j.cell.2017.09.030.

- 1 87. Nguyen, L.T., Schmidt, H.A., von Haeseler, A., and Minh, B.Q. (2015). IQ-TREE: a fast and
2 effective stochastic algorithm for estimating maximum-likelihood phylogenies. *Mol. Biol. Evol.* 32,
3 268-274. 10.1093/molbev/msu300.
- 4 88. Letunik, I, and Bork, P. (2021). Interactive Tree Of Life (iTOL) v5: an online tool for phylogenetic
5 tree display and annotation. *Nuc. Acid Res.* 10.1093/nar/gkab301.
- 6 89. R Core Team (2020). R: A language and environment for statistical computing. (R Foundation for
7 Statistical Computing). <https://www.R-project.org/>.
- 8 90. Fox, J., and Weisberg, S. (2019). *An R Companion to Applied Regression*, Third edition (Sage).
- 9 91. Shapiro, S.S., and Wilk, M.B. (1965). An analysis of variance test for normality (complete samples).
10 *Biometrika* 52, 591-611. 10.1093/biomet/52.3-4.591.
- 11 92. Levene, H. (1960). Robust tests for equality of variances. In *Contributions to Probability and*
12 *Statistics*, I. Olkin, ed. (Stanford Univ. Press), pp. 278-292.
- 13 93. Benjamini, Y., and Hochberg, Y. (1995). Controlling the false discovery rate: a practical and
14 powerful approach to multiple testing. *J. Roy. Stat. Soc. B. Met.* 57, 289-300. 10.1111/j.2517-
15 6161.1995.tb02031.x.
- 16 94. Wickham, H. (2016). *ggplot2: Elegant Graphics for Data Analysis* (Springer-Verlag New York).
- 17 95. Patro, R., Duggal, G., Love, M.I., Irizarry, R.A., and Kingsford, C. (2017). Salmon provides fast and
18 bias-aware quantification of transcript expression. *Nature Methods* 14, 417-419. 10.1038/nmeth.4197.
- 19 96. Love, M.I., Huber, W., and Anders, S. (2014). Moderated estimation of fold change and dispersion
20 for RNA-seq data with DESeq2. *Genome Biology* 15, 550. 10.1186/s13059-014-0550-8.
- 21 97. Heberle, H., Meirelles, G.V., da Silva, F.R., Telles, G.P., and Minghim, R. (2015). InteractiVenn: a
22 web-based tool for the analysis of sets through Venn diagrams. *BMC Bioinformatics* 16, 169.
23 10.1186/s12859-015-0611-3.
- 24 98. Conway, J.R., Lex, A., and Gehlenborg, N. (2017). UpSetR: an R package for the visualization of
25 intersecting sets and their properties. *Bioinformatics* 33, 2938-2940. 10.1093/bioinformatics/btx364.

1 KEY RESOURCES TABLE

REAGENT or RESOURCE	SOURCE	IDENTIFIER
Antibodies		
Bacterial and Virus Strains		
Biological Samples		
Chemicals, Peptides, and Recombinant Proteins		
C-fern 1% agar (pH6.0) growth media	55	N/A
Sodium hypochlorite	Fisher Scientific	CAS 7681-52-9 Cat#11448842
Abscisic acid (ABA)	Sigma Aldrich	CAS 14375-45-2 Cat#A1049
2-(N-Morpholino)ethanesulfonic acid (MES)	Sigma Aldrich	CAS 4432-31-9 Cat#M3671
Tween20	Fisher Scientific	CAS 9005-64-5 Cat#11417160
KOH	Fisher Scientific	CAS 1310-58-3 Cat#437135000
Ethanol	Fisher Scientific	CAS 64-17-5 Cat#16688242
Critical Commercial Assays		
RNeasy Plant mini kit	QIAGEN	Cat#74904
RNase-free DNase	QIAGEN	Cat#79254
Bioanalyzer RNA 6000 pico assay	Agilent	Cat#5067-1513
TruSeq RNA library prep kit V2	Illumina Systems	Cat#RS-122-2001
KAPA library quantification kit	Roche	Cat#KR0405
NextSeq 500/550 High Output kit (150 cycles)	Illumina Systems	Cat#20024907
Deposited Data		
Raw sequence reads	This paper	NCBI SRA: SAMN16306556
Assembled transcriptome	This paper	NCBI TSA: PRJNA666635
Protein-coding sequences (predicted)	This paper	Figshare: https://doi.org/10.6084/m9.figshare.13807967
Experimental Models: Cell Lines		
Experimental Models: Organisms/Strains		
<i>Ceratopteris richardii</i> , strain Hn-n	54	N/A
Oligonucleotides		

Recombinant DNA		
Software and Algorithms		
QCapture Pro (version 7)	Teledyne Photometrics	RRID:SCR_014432; http://www.qimaging.com/products/software/qcappro7.php
Fiji (version 1.52s)	57	RRID:SCR_002285; http://fiji.sc
Photoshop 2019 (version 21.2.5)	Adobe	RRID:SCR_014199; https://www.adobe.com/products/photoshop.html
rCorrector (version 1.0.4-2)	58	https://github.com/mourisl/Rcorrector
FilterUncorrectablePEfastq (version e2df226, 19th Feb 2019)	Harvard FAS Informatics	https://github.com/harvardinformatics/TranscriptomeAssemblyTools
TrimGalore (version 0.6.0)	Babraham Institute	https://www.bioinformatics.babraham.ac.uk/projects/trim_galore
Cutadapt (version 2.8)	59	RRID:SCR_011841; https://cutadapt.readthedocs.org/
FastQC (version 0.11.8)	60	RRID:SCR_014583; http://www.bioinformatics.babraham.ac.uk/projects/fastqc/
Bowtie2 (version 2.3.5.1)	62	RRID:SCR_016368 ; http://bowtie-bio.sourceforge.net/bowtie2/index.shtml
Trinity (version 2.9.0)	63	RRID:SCR_013048; https://github.com/trinityrnaseq/trinityrnaseq
Salmon (version 1.1.0)	95	RRID:SCR_017036; https://combine-lab.github.io/salmon/
DESeq2 (version 1.18.1)	96	RRID:SCR_015687; https://bioconductor.org/packages/release/bioc/html/DESeq2.html
Transdecoder (version 5.5.0)	http://transdecoder.sf.net	RRID:SCR_017647; https://github.com/TransDecoder/TransDecoder
InteractiVenn	97	http://www.interactivenn.net/

GeneMark-ES (version 5.1)	64	RRID:SCR_011930; http://opal.biology.gatech.edu/GeneMark/
OrthoFinder (version 2.3.11)	78	RRID:SCR_017118; https://github.com/davidemms/OrthoFinder
BUSCO (version 5.2.1)	83	RRID:SCR_015008; http://busco.ezlab.org/
The Arabidopsis Information Resource (TAIR10)	65	RRID:SCR_001901; https://www.arabidopsis.org/
Phytozome (version 13)	77	https://phytozome-next.jgi.doe.gov/
MAFFT (version 7.427)	http://mafft.cbrc.jp/alignment/server	RRID:SCR_011811
IQ-TREE (version 2.1.3)	87	RRID:SCR_017254; http://www.iqtree.org
Interactive Tree of Life (iTOL) (version 6)	88	RRID:SCR_018174; https://itol.embl.de
R (version 3.6.3)	89	https://www.r-project.org/
R package: Car (version 3.0-7)	90	https://cran.r-project.org/web/packages/car/index.html
R package: ggplot2 (version 3.3.0)	94	RRID:SCR_014601; https://cran.r-project.org/web/packages/ggplot2/index.html
R package: UpSetR (version 1.4.0)	98	https://cran.r-project.org/web/packages/UpSetR/index.html
Other		
TinyTag Plus2 data logger	Gemini Data Loggers	Cat#TGP-4017
Olympus BX51 transmitted light microscope	Olympus Corporation	N/A
Agilent 2100 Bioanalyzer	Agilent	Cat#G2939BA
HiSeq2000 high throughput genetic sequencer	Illumina Systems	RRID:SCR_020132
SILVA rRNA SSUParc database, release 132	61	N/A
SILVA LSUParc database, release 132	61	N/A
Reference genome, <i>Amborella trichopoda</i> (v1.0)	66	https://phytozome-next.jgi.doe.gov/info/Atrichopoda_v1_0
Reference genome, <i>Glycine max</i> (Wm82.a4.v1)	67	https://phytozome-next.jgi.doe.gov/info/Gmax_Wm82_a4_v1
Reference genome, <i>Manihot esculenta</i> (v7.1)	68	https://phytozome-next.jgi.doe.gov/info/Mesculenta_v7_1
Reference genome, <i>Micromonas pusilla</i> strain CCMP1545 (v3.0)	69	https://phytozome-next.jgi.doe.gov/info/MpusillaCCMP1545_v3_0
Reference genome, <i>Ostreococcus lucimarinus</i> (v2.0)	70	https://phytozome-next.jgi.doe.gov/info/Olucimarinus_v2_0
Reference genome, <i>Oryza sativa</i> (v7.0)	71	https://phytozome-next.jgi.doe.gov/info/Osativa_v7_0

Reference genome, <i>Physcomitrella patens</i> (v3.3)	72	https://phytozome-next.jgi.doe.gov/info/Ppatens_v3_3
Reference genome, <i>Solanum lycopersicum</i> (ITAG3.2)	73	https://phytozome-next.jgi.doe.gov/info/Slycopersicum_ITAG3_2
Reference genome, <i>Selaginella moellendorffii</i> (v1.0)	74	https://phytozome-next.jgi.doe.gov/info/Smoellendorffii_v1_0
Reference genome, <i>Spirodela polyrhiza</i> (v2)	75	https://phytozome-next.jgi.doe.gov/info/Spolyrhiza_v2
Reference genome, <i>Volvox carteri</i>	76	https://phytozome-next.jgi.doe.gov/info/Vcarteri_v2_1
Reference genome, <i>Marchantia polymorpha</i> (v3.1)	86	https://phytozome-next.jgi.doe.gov/info/Mpolymorpha_v3_1
Gene annotation library, Gene Ontology	79, 80	RRID:SCR_002811
Gene annotation library, Plant Ontology	81	RRID:SCR_006494
Gene annotation library, MapMan	82	RRID:SCR_005060

FIGURES

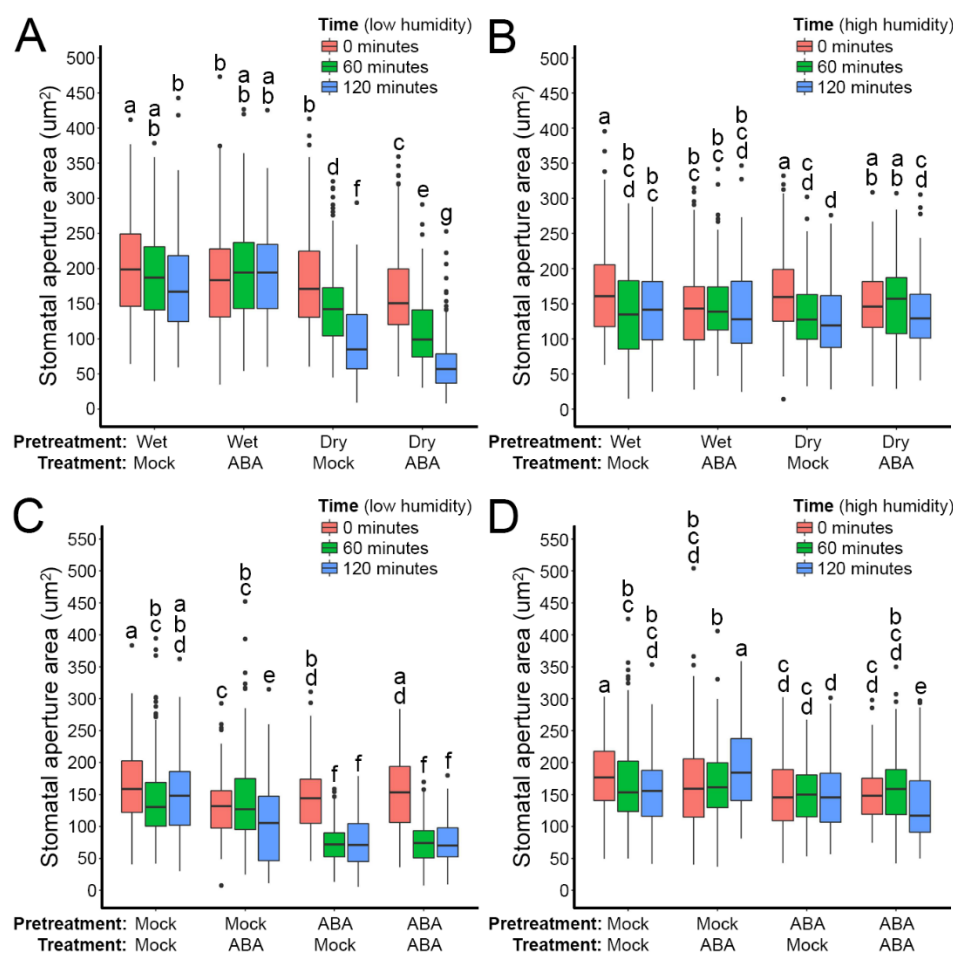


Figure 1. Active closure of *C. richardii* stomata in response to low humidity and ABA is conditional on pre-exposure to either stimulus.

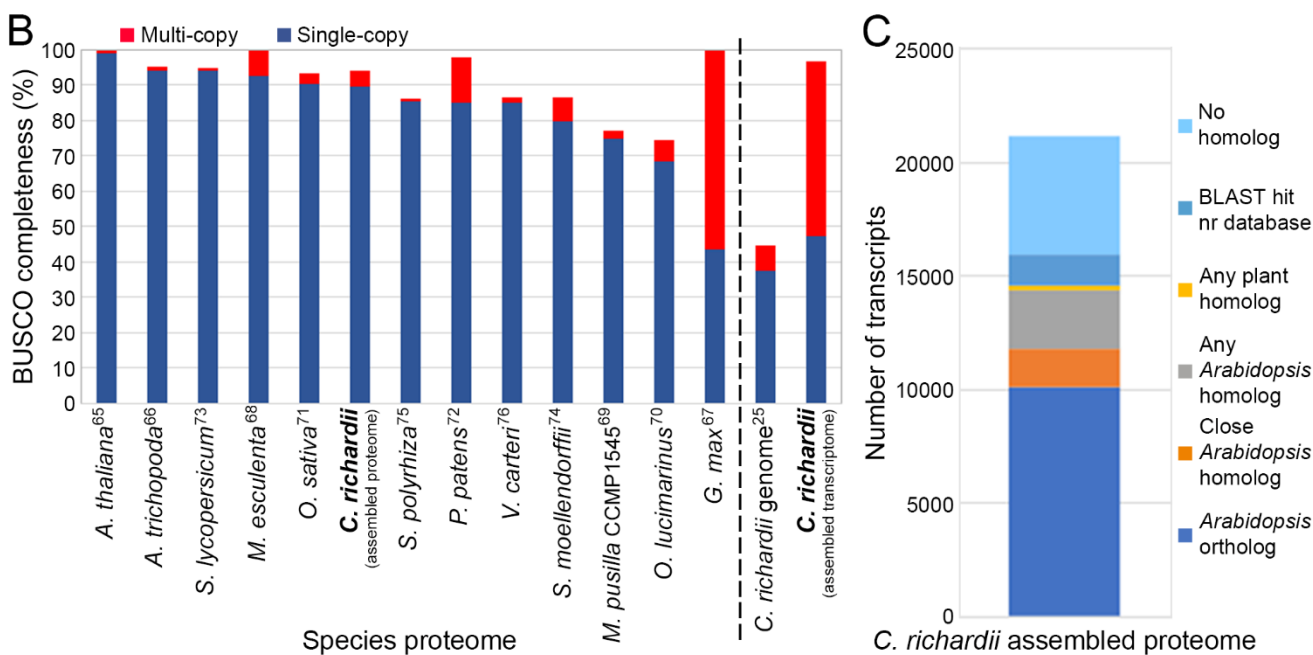
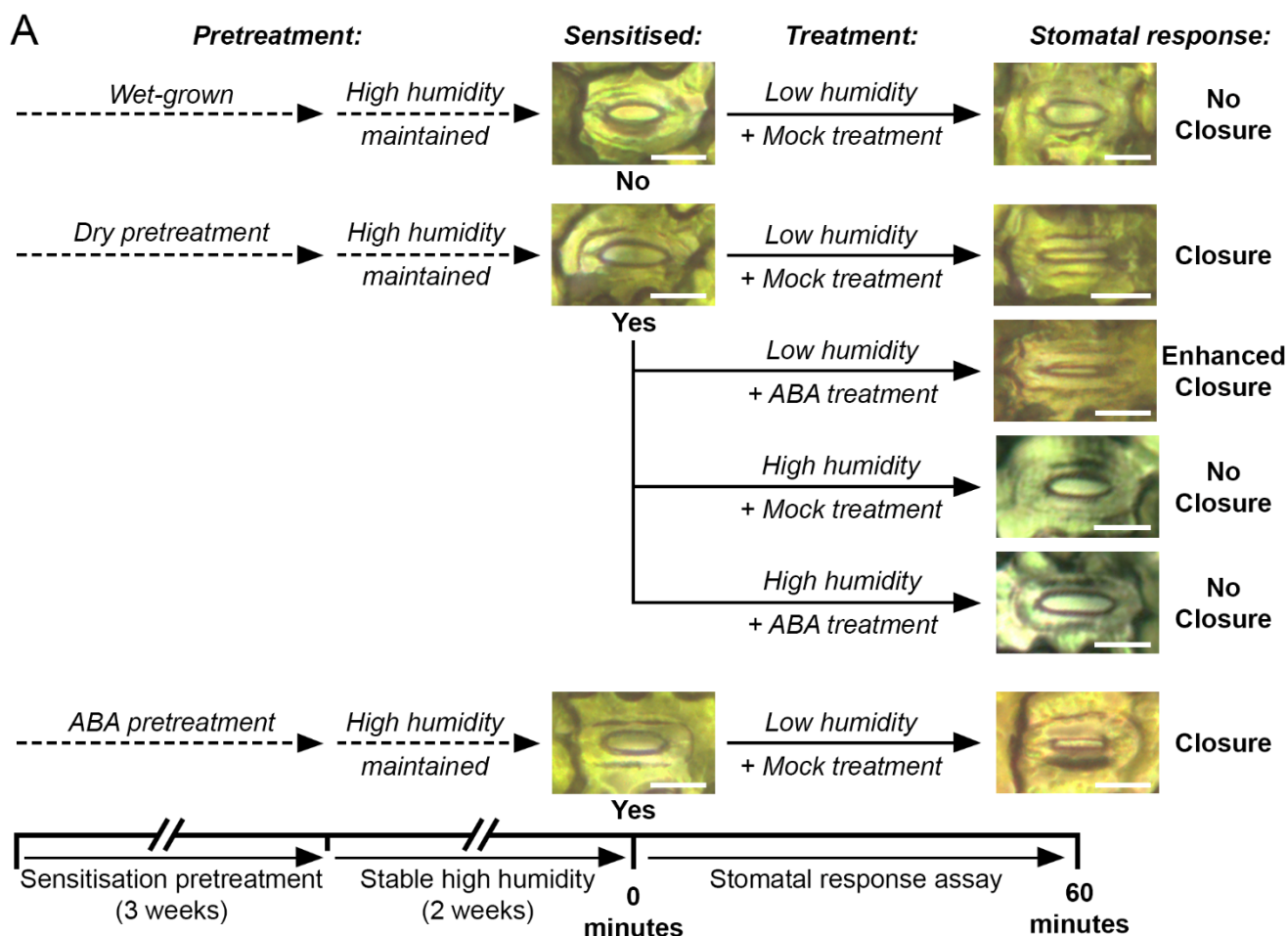
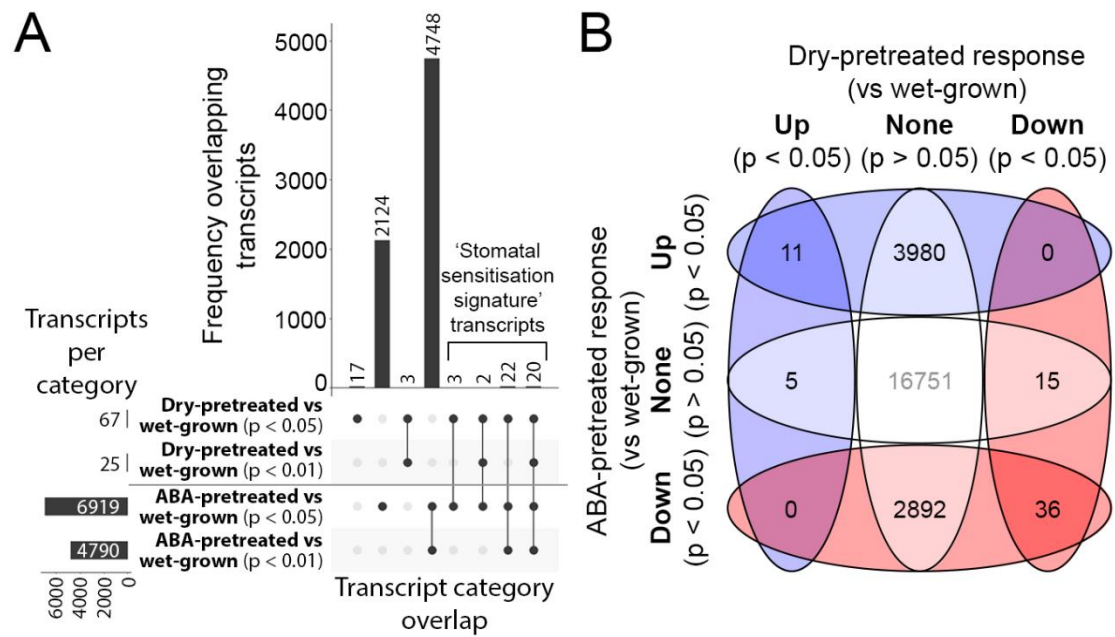


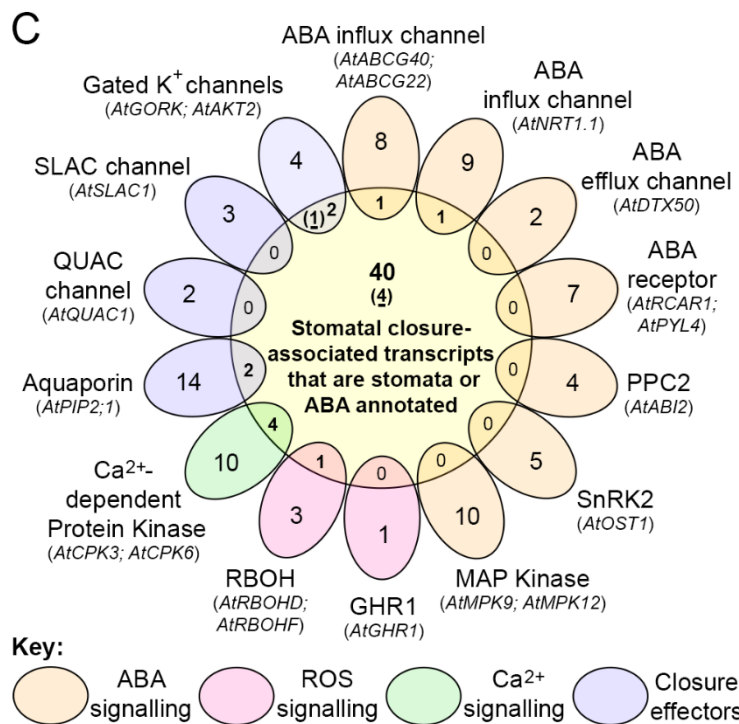
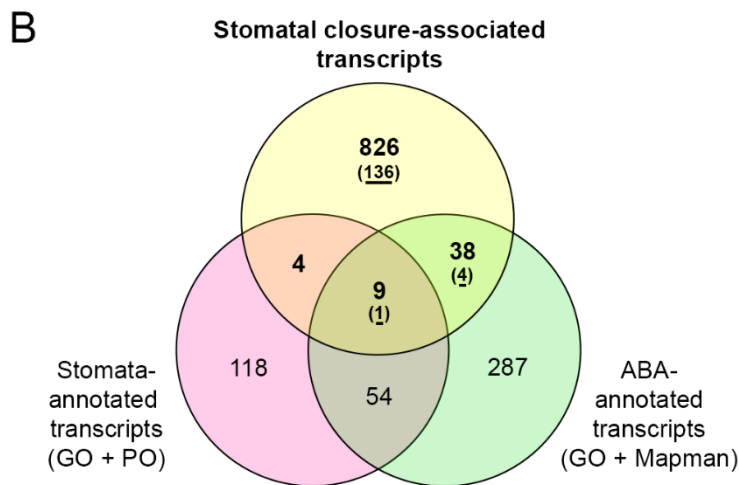
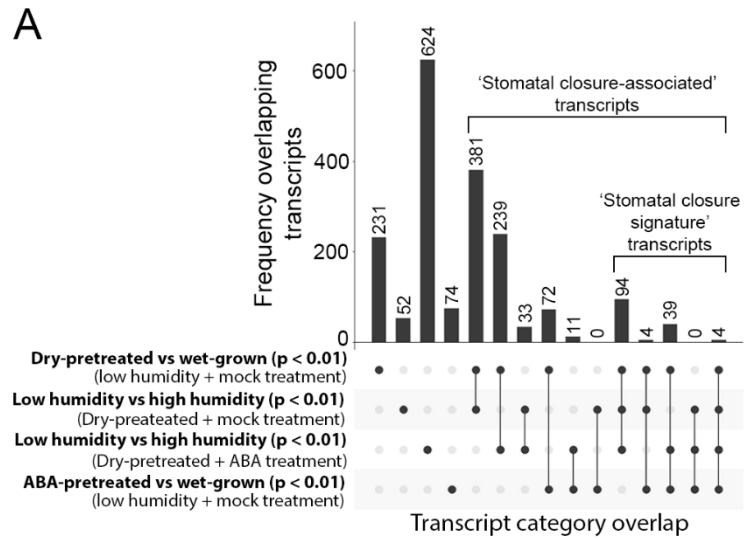
Figure 2. De novo transcriptome assembly provides a robust platform for the identification of stomatal sensitisation and closure signatures.



1

2 **Figure 3. Shared transcriptomic responses in both dry-pretreated and ABA-pretreated *C.***

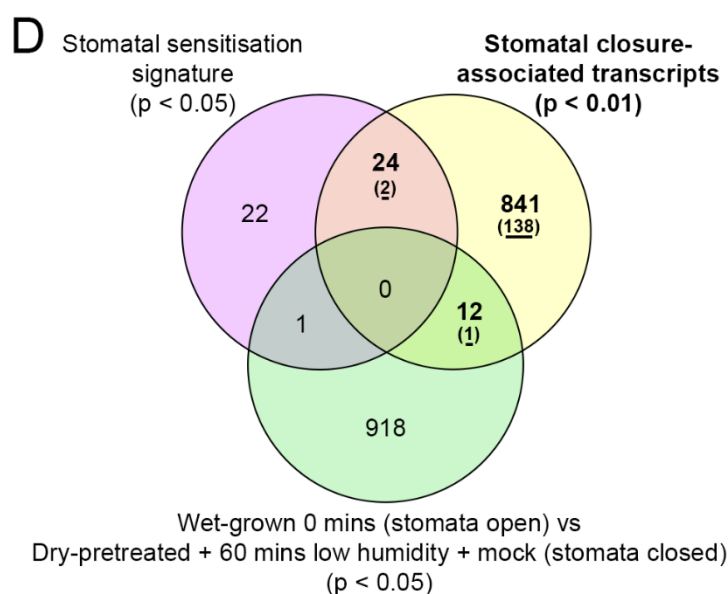
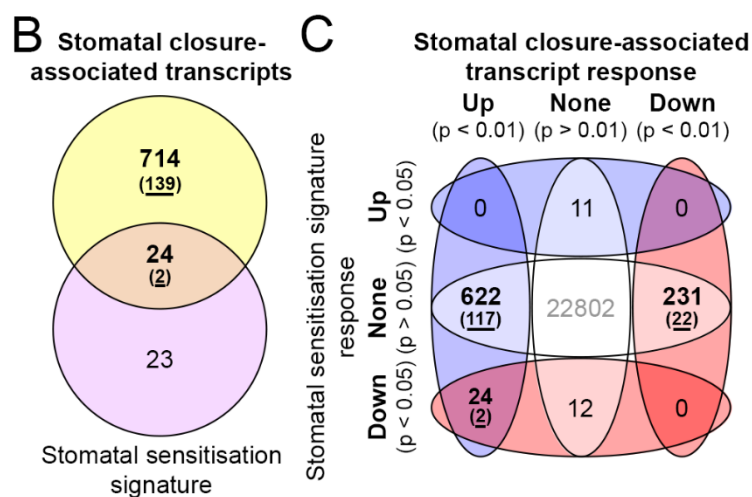
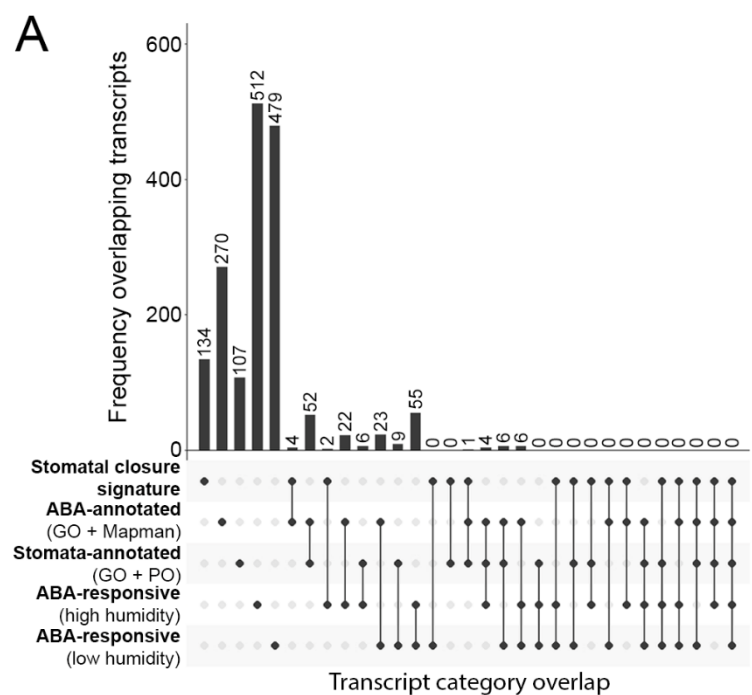
3 ***richardii* fronds reflect a common underlying sensitisation process.**



1

2 **Figure 4. Homologs of genes underlying stomatal closure in *Arabidopsis* are also associated**

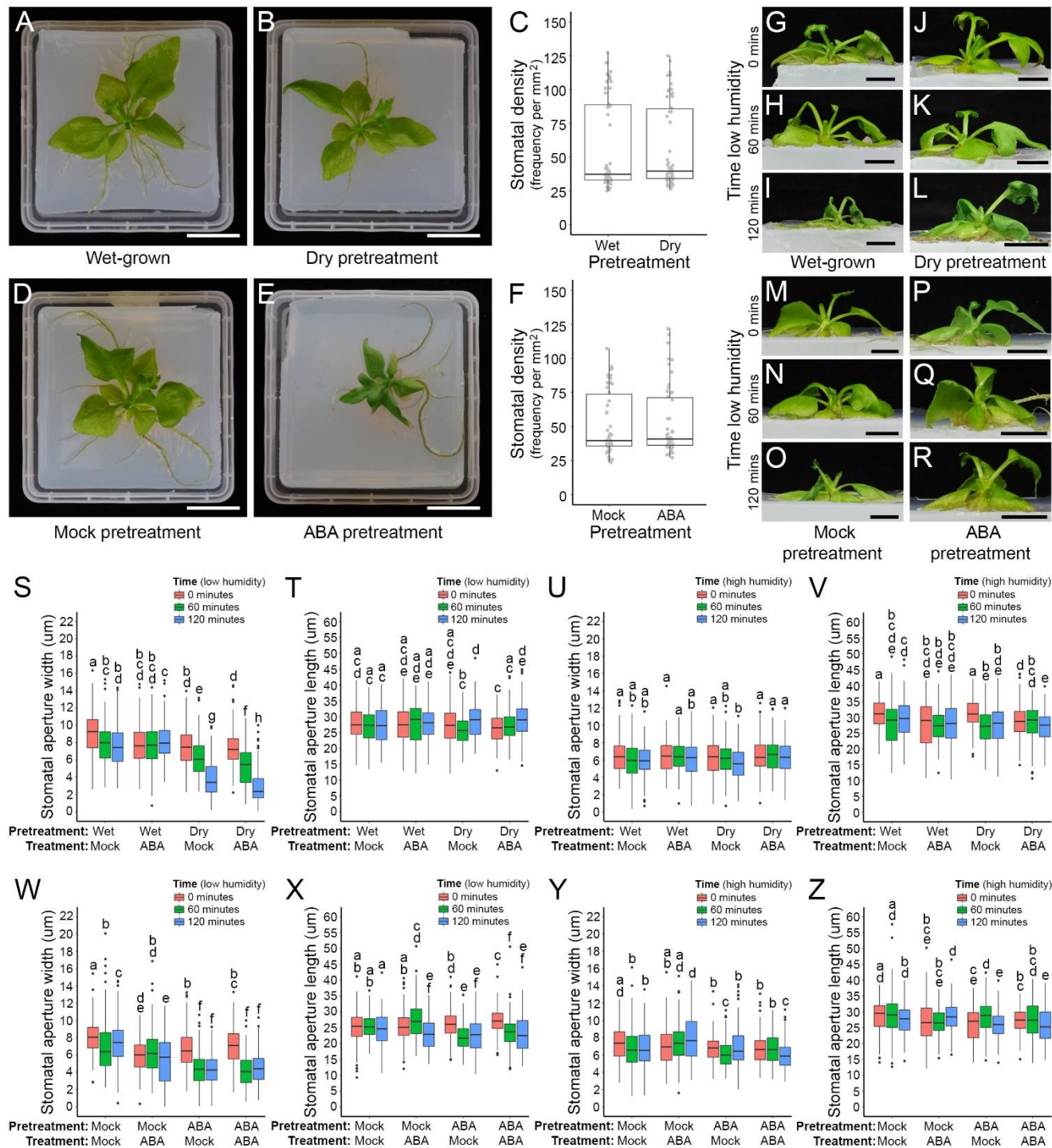
3 **with closure in *C. richardii*.**



1

2 **Figure 5. Transcriptome profiles during stomatal closure and sensitisation suggest shared but**
3 **opposing regulatory mechanisms that are largely ABA-independent.**

1 **SUPPLEMENTAL FIGURES AND TABLES**



2 **Figure S1. Pretreatment effects on *C. richardii* whole plant phenotypes and stomatal linear**
3 **measurements, Related to Figure 1.**

4 (A-C) Effect of dry pretreatment on whole plant morphology. (A and B) Morphology of 50 day-old wet-
5 grown (A) and dry-pretreated (B) plants at 0 minutes exposure to low humidity. Scale bars = 20 mm.
6 (C) Stomatal density on fronds from wet-grown or dry-pretreated plants used for stomatal response
7 assays in **Figures 1A and 1B**. *n* = 18 independent plants, 3 density measurements taken across a
8

1 single frond lamina per plant. Boxplots represent the 25th-75th percentile (box), the median value (mid-
2 line) and up to 1.5x of the interquartile range (whiskers).

3 **(D-F)** Effect of ABA pretreatment on whole plant morphology. **(D and E)** Morphology of 50 day-old wet-
4 grown plants pretreated with mock solution **(D)** or 100 μ M ABA **(E)** at 0 minutes exposure to low
5 humidity. Scale bars = 20 mm. **(F)** Stomatal density on fronds from mock- or ABA-pretreated plants
6 used for stomatal response assays in **Figures 1C and 1D**. $n = 18$ independent plants, 3 density
7 measurements taken across a single frond lamina per plant. Boxplots represent the 25th-75th percentile
8 (box), the median value (mid-line) and up to 1.5x of the interquartile range (whiskers).

9 **(G-R)** Whole plant phenotypes of wet-grown **(G-I)**, dry-pretreated **(J-L)**, mock-pretreated **(M-O)** and
10 ABA-pretreated plants **(P-R)** at 0, 60 and 120 minutes after transfer to low humidity from stable high
11 humidity and treated with mock solution at 0 minutes by foliar spray. Scale bars = 10 mm.

12 **(S-Z)** Linear stomatal dimensions from stomatal response assays (**Figure 1**), comparing wet-grown
13 ('Wet') versus dry-pretreated ('Dry') plants **(S-V)** and wet-grown plants pretreated with periodic
14 exogenous application of 100 μ M ABA ('ABA') versus corresponding mock solution ('Mock') **(W-Z)** (see
15 STAR Methods). Fronds were either exposed to low (ambient) humidity **(S,T,W,X)** or maintained in
16 high humidity conditions **(U,V,Y,Z)**. Dimensions shown are stomatal width (distance between the
17 midpoint of the two guard cells) **(S,U,W,Y)** and length (distance between the points where the guard
18 cells attach) **(T,V,X,Z)**. $n = 180$ stomata per pretreatment + treatment combination, measured from
19 three independent plants per timepoint. Boxplots represent the 25th-75th percentile (box), the median
20 value (mid-line) and up to 1.5x of the interquartile range (whiskers). Pairwise comparisons were
21 performed using two-tailed Mann-Whitney tests because stomatal linear measurement data did not
22 meet the assumptions of ANOVA (see STAR Methods). Where necessary to meet the assumptions of
23 the Mann-Whitney test, comparisons were performed on square-root **(W,X,Y)** or log₁₀-transformed
24 datasets **(Z)**. Letters denote statistically significant differences ($p < 0.05$) within each plot.
25 Pretreatment+treatment combinations with the same letter are not significantly different from each
26 other. All individual stomatal measurements are provided in **Data S1B-E**.

27
28

Phylogenetic trees showing the relationship of *C. richardii* transcripts within orthogroups containing the ABCG (A), ABCC (B), and GRDP (C) gene families. The numbers shown represent bootstrap support for each node. Green boxes denote *Arabidopsis* genes with stomatal-related functions, yellow boxes denote *C. richardii* transcripts identified as sensitisation signature transcripts (Data S2A). Asterisks in (A) denote *Arabidopsis* homologs with published ABA transporter capability. In (C), whilst the median protein sequence length was 763 amino acids, four sequences within the orthogroup (TRINITY_DN3590_c0_g2, TRINITY_DN16455_c0_g1, TRINITY_DN6624_c0_g1, At4g37682.1) were less than 80 aa and as such their phylogenetic positions should be treated with caution.

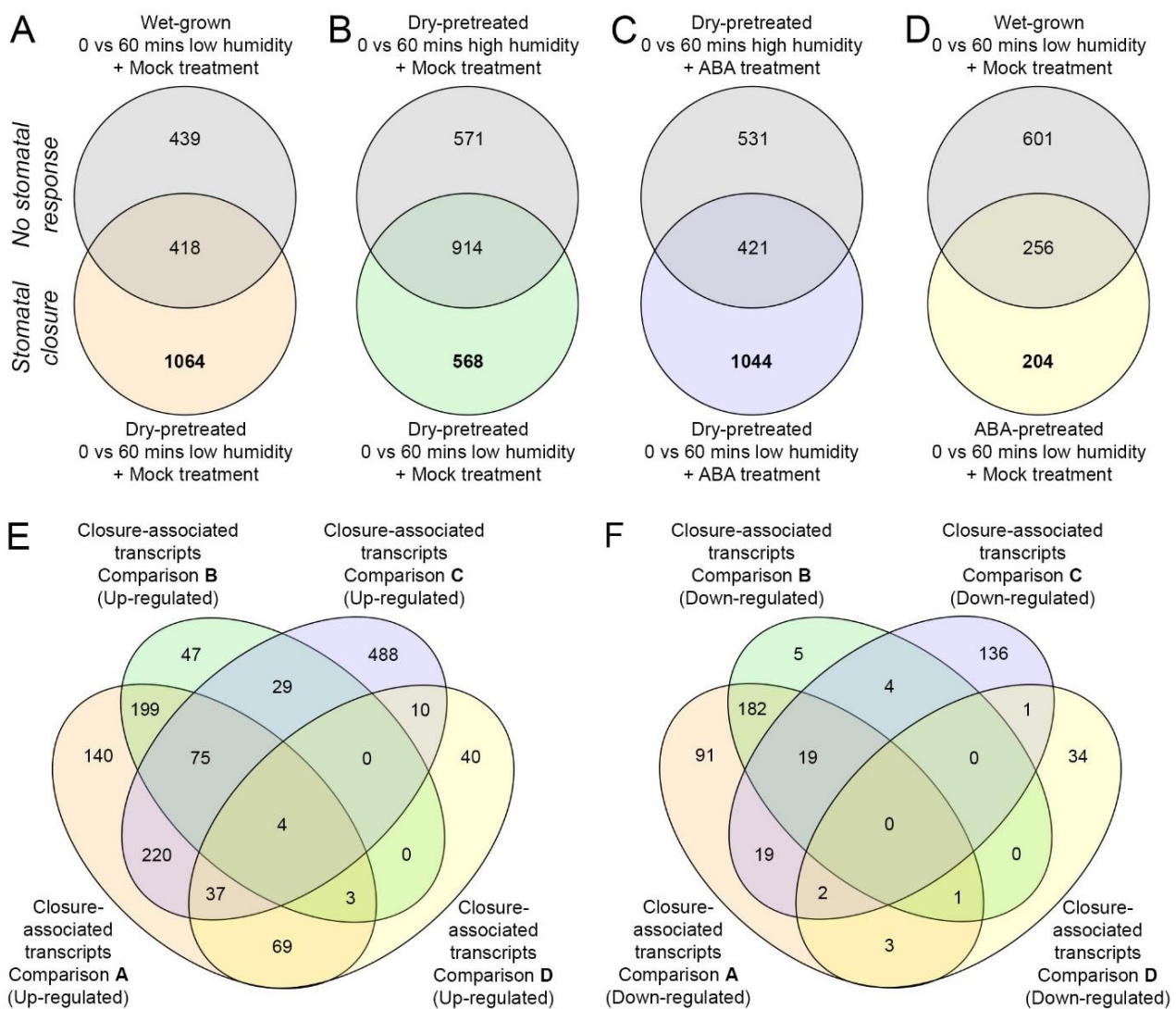


Figure S3. Transcriptome changes associated with stomatal closure in *C. richardii*, Related to Figure 4.

(A-D) Venn comparisons of transcripts that accumulated to significantly different levels ($p < 0.01$) in stomatal response assays. For each assay, transcripts with significantly different abundance levels (p

1 < 0.01) between 0 and 60 minute samples were identified. This revealed significant differences for: 857
2 transcripts in wet-grown + low humidity & Mock treated samples; 1485 in dry-pretreated + high humidity
3 & Mock treated; 952 in dry-pretreated + high humidity & ABA treated; 1482 in dry-pretreated + low
4 humidity & Mock treated; 1465 in in dry-pretreated + low humidity & ABA treated; and 460 in ABA-
5 pretreated + low humidity & Mock treated (**Data S3D-I**). Populations of transcripts with significantly
6 different abundance levels were then compared between pairs of assays (**A-D**) such that environmental
7 and/or pretreatment conditions were as similar as possible but stomatal closure was represented in
8 only one assay within each pair (non-grey circle in each case). Transcripts with significantly different
9 abundance levels only in the assay involving stomatal closure were inferred to be candidate stomatal
10 closure transcripts. Environmental conditions and sensitisation status pertaining to each assay are as
11 shown.

12 (**E** and **F**) Venn comparisons of transcripts associated with stomatal closure, comparing transcripts up-
13 regulated (**E**) and down-regulated (**F**) for each dataset identified in (**A-D**). The sum of each Venn
14 category between (**E**) and (**F**) corresponds to the equivalent Upset category in **Figure 4A**. Individual
15 transcript identities are provided in **Data S3A**.

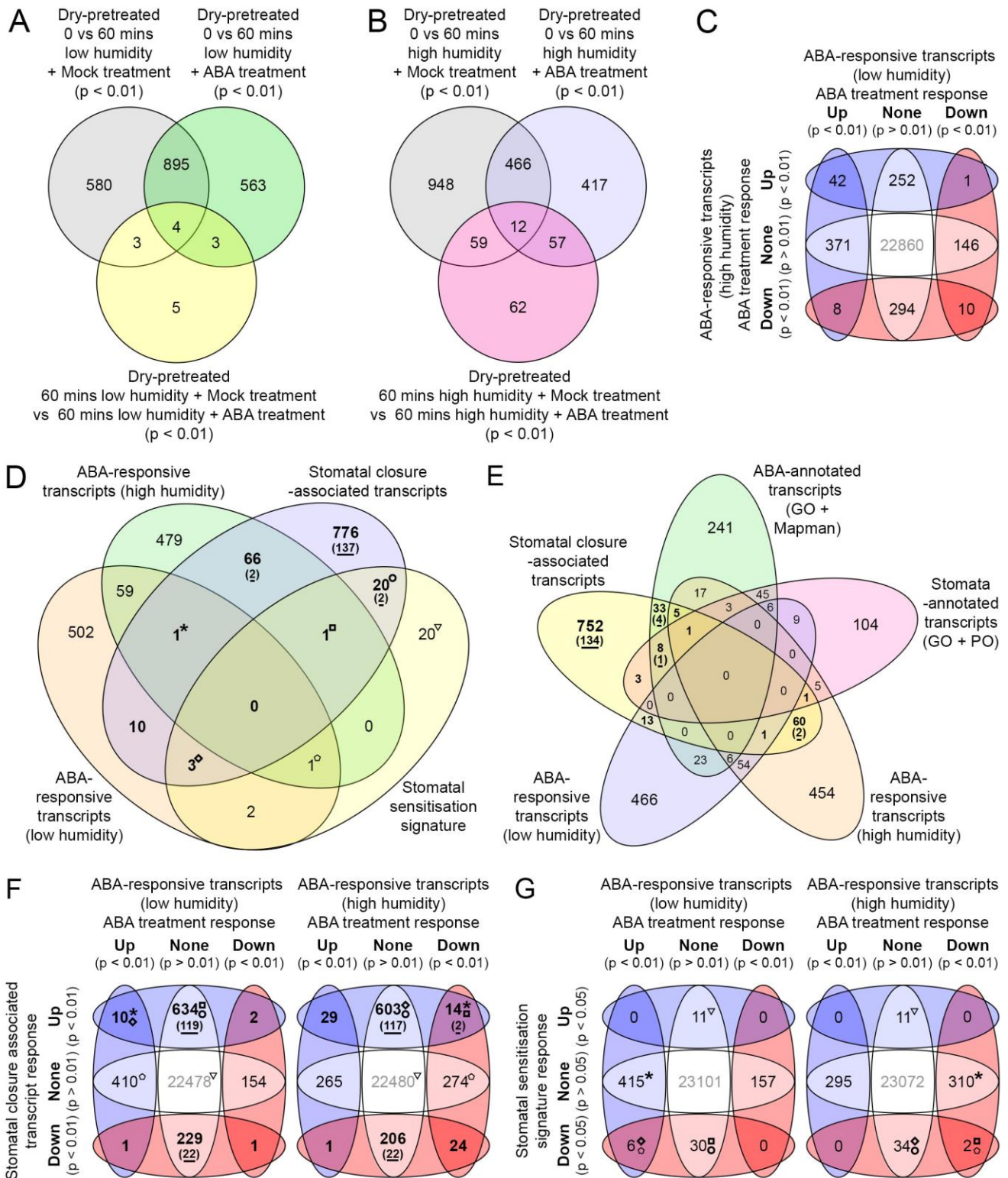


Figure S4. Humidity-dependent ABA responses of stomatal closure-associated and sensitisation signature transcripts, Related to Figure 5.

(A and B) Venn comparison between transcript changes in fronds after 60 minutes mock and ABA treatment under low humidity (A) and high humidity (B). Transcripts which showed a significant change in abundance ($p < 0.01$) in ABA-treated fronds but not mock-treated fronds, or which showed a significant difference in abundance ($p < 0.01$) between mock and ABA-treated fronds after 60 minutes

1 were classified as ABA-responsive. Identities of individual ABA-responsive transcripts are given in
2 **Data S4A**, and identities of individual transcripts within each category are given in **Data S3E-H** and
3 **Data S4D-E**.

4 **(C)** Venn comparison of directional changes in level of ABA-responsive transcripts (**A** and **B**) after ABA
5 treatment under low and high humidity. The majority of shared transcripts show similar directional
6 responses to ABA treatment under both humidity conditions.

7 **(D)** Venn comparison between stomatal closure-associated transcripts, stomatal sensitisation
8 signature transcripts and all ABA-responsive transcripts under low or high humidity (**A** and **B**).
9 Superscript symbols denote categories of interest. One closure-associated transcript is ABA-
10 responsive under both low and high humidity (asterisk), as is a single transcript specific to the
11 sensitisation signature (pentagon). Three transcripts common to both the closure-associated and
12 sensitisation datasets are ABA-responsive under low humidity (diamond) while a fourth is ABA-
13 responsive under high humidity (square). The ABCG homolog identified within the sensitisation
14 signature (open circle) is also a closure-associated transcript, but neither this nor the AtMRP4 ortholog
15 (open triangle) are ABA-responsive. Individual identities of the transcripts within each category are
16 provided in **Data S4B**.

17 **(E)** Venn comparison between stomatal closure-associated transcripts (**bold**), all transcripts with
18 annotations relating to ABA and stomata functions, and all ABA-responsive transcripts under low or
19 high humidity (**A** and **B**). Underlined numbers given in brackets denote closure signature transcripts
20 from within the closure-associated transcript dataset. Individual identities of ABA-responsive
21 ABA/stomata-annotated transcripts are provided in **Data S4C**.

22 **(F and G)** Venn comparison between the abundance changes of either stomatal closure-associated
23 transcripts (**F**, **bold**) or stomatal sensitisation signature transcripts (**G**) during ABA treatment under low
24 and high humidity. Superscript symbols within a response category correspond to the categories
25 identified in **(D)**. The single closure-associated transcript responsive to ABA under both low and high
26 humidity (asterisk) increases abundance during closure and is similarly regulated by ABA under low
27 humidity. Under high humidity, however, abundance is decreased after ABA treatment (**F**). Conversely,
28 the single sensitisation signature transcript that is responsive to ABA under both humidity conditions
29 (pentagon) shows opposite abundance changes between sensitisation and ABA treatment under low

humidity but similar changes between sensitisation and ABA treatment under high humidity (**G**). The abundance of the ABCG homolog (open circle) responds oppositely to closure and sensitisation (**F** and **G**).

In (**D**), (**E**) and (**F**), values in bold denote stomatal closure-associated transcripts, and underlined values in brackets denote stomatal closure signature transcripts within each category.

1

BUSCO dataset	Embryophyta_odb9					Eukaryote_odb9				
	Complete	Single	Duplicated	Fragments	Missing	Complete	Single	Duplicated	Fragments	Missing
Geng <i>et al.</i> 2021 assembly ^{S1}	71.0%	43.0%	28.0%	3.0%	27.0%	97.0%	52.0%	45.0%	1.0%	2.0%
Plackett <i>et al.</i> assembly (raw)	84.5%	37.9%	46.6%	2.7%	12.8%	98.0%	44.3%	53.7%	1.6%	0.4%
Plackett <i>et al.</i> assembly (expressed isoforms only)	81.3%	36.0%	45.3%	16.7%	16.7%	94.9%	42.0%	52.9%	0.8%	4.3%

2

3 **Table S1. Comparative BUSCO analysis between *C. richardii de novo* transcriptome**
4 **assemblies, Related to Figure 2.**

5 Analysis compares the assembly generated in this study against a previously-published *de novo*
6 assembly^{S1}, using the same benchmarking datasets as for the previously-published assembly.

7

Gene family	Representative <i>Arabidopsis</i> homolog	Homologous <i>C. richardii</i> Transcript ID
ABC transporter (ABA influx)	ABCG40 (At1g15520)	TRINITY_DN6545_c1_g2
		TRINITY_DN1286_c0_g1
		TRINITY_DN94_c0_g1
		TRINITY_DN7811_c0_g1
		TRINITY_DN7654_c0_g1
		TRINITY_DN7162_c0_g1
	ABCG22 (At5g06530)	TRINITY_DN9036_c0_g1
		TRINITY_DN5116_c0_g1
NRT/PTR/AIT (ABA influx)	NRT1.1 (At1g12110)	TRINITY_DN7391_c0_g1
		TRINITY_DN451_c1_g1
		TRINITY_DN16308_c0_g1
		TRINITY_DN1363_c1_g2
		TRINITY_DN1591_c0_g1
		TRINITY_DN8424_c0_g1
		TRINITY_DN5410_c0_g1
		TRINITY_DN6774_c0_g1
		TRINITY_DN4480_c0_g1
		TRINITY_DN788_c0_g1
DTX (ABA efflux)	DTX50 (At5g52050)	TRINITY_DN5662_c1_g1
		TRINITY_DN5838_c1_g1
		TRINITY_DN4936_c0_g1

PYR/PYL/RCAR (ABA receptor)	RCAR1 (At1g01360)	TRINITY_DN59389_c0_g1
		TRINITY_DN8764_c0_g1
		TRINITY_DN2390_c0_g1
	PYL4 (At2g38310)	TRINITY_DN2357_c0_g1
		TRINITY_DN544_c3_g3
		TRINITY_DN5040_c0_g1
PP2C (ABA signalling)	ABI2 (At5g57050)	TRINITY_DN6722_c0_g1
		TRINITY_DN1770_c0_g1
		TRINITY_DN385_c1_g1
		TRINITY_DN3232_c0_g2
SnRK2	OST1 (At4g33950)	TRINITY_DN381_c0_g2
		TRINITY_DN8240_c0_g2
		TRINITY_DN6331_c1_g1
		TRINITY_DN17670_c0_g1
		TRINITY_DN17670_c0_g2
CPK (calcium-dependent protein kinase)	CPK3 (At4g23650)	TRINITY_DN438_c0_g3
		TRINITY_DN7763_c0_g1
		TRINITY_DN438_c0_g1
		TRINITY_DN232_c0_g1
		TRINITY_DN438_c0_g2
	CPK6 (At2g17290)	TRINITY_DN6531_c1_g1
		TRINITY_DN3253_c1_g1
		TRINITY_DN7498_c0_g1
		TRINITY_DN108_c0_g1
		TRINITY_DN71816_c0_g1
		TRINITY_DN2453_c1_g1
		TRINITY_DN6531_c2_g1
		TRINITY_DN6531_c2_g2
		TRINITY_DN4788_c0_g1
MPK (MAP protein kinase)	MPK9 (At3g18040)	TRINITY_DN605_c0_g2
		TRINITY_DN209_c0_g1
		TRINITY_DN605_c0_g1
		TRINITY_DN6721_c1_g1
		TRINITY_DN6287_c0_g1
		TRINITY_DN2793_c0_g1
		TRINITY_DN8052_c0_g1
		TRINITY_DN12151_c0_g2
	MPK12 (AT2G46070)	TRINITY_DN4359_c0_g1
		TRINITY_DN4263_c0_g1
GHR1	GHR1 (At4g20940)	TRINITY_DN9295_c0_g1
RBOH (ROS signalling)	RBOHD (At5g47910)	TRINITY_DN882_c0_g1
		TRINITY_DN9319_c0_g1
		TRINITY_DN2856_c0_g1
		TRINITY_DN2783_c0_g1

Aquaporin (water channel)	PIP2;1 (AT3G53420)	TRINITY_DN77350_c0_g1
		TRINITY_DN23501_c0_g1
		TRINITY_DN23501_c0_g2
		TRINITY_DN72249_c0_g1
		TRINITY_DN9477_c0_g1
		TRINITY_DN64006_c1_g1
		TRINITY_DN6156_c2_g2
		TRINITY_DN44957_c0_g1
		TRINITY_DN13276_c1_g2
		TRINITY_DN39145_c0_g2
		TRINITY_DN57940_c0_g1
		TRINITY_DN6156_c2_g1
		TRINITY_DN39145_c0_g1
		TRINITY_DN60742_c0_g1
		TRINITY_DN13276_c3_g1
		TRINITY_DN77350_c2_g1
S-type anion channel	SLAC1 (At1g12480)	TRINITY_DN12013_c0_g1
		TRINITY_DN6137_c1_g1
		TRINITY_DN3264_c0_g1
R-type anion channel	QUAC1 (At4g17970)	TRINITY_DN5940_c0_g2
		TRINITY_DN5940_c0_g2
SHAKER voltage-gated K ⁺ channel	GORK (At5g37500)	TRINITY_DN2798_c0_g1
		TRINITY_DN51_c0_g1
	AKT2 (At4g22200)	TRINITY_DN1642_c1_g1
		TRINITY_DN7588_c0_g1
		TRINITY_DN3571_c0_g1
		TRINITY_DN3309_c2_g1

Table S2. *C. richardii* transcripts orthologous to selected *Arabidopsis* stomatal closure genes, Related to Figure 4.

All *C. richardii* transcripts within the assembled transcriptome with orthology to *Arabidopsis* genes with known functions in stomatal closures (as shown). Orthologs to specific *Arabidopsis* genes were determined using the outputs of the Orthofinder analysis conducted (see STAR Methods).

SUPPLEMENTAL REFERENCE

^{S1}Geng, Y., Cai, C., McAdam, S.A.M., Banks, J.A., Wisecaver, J.H., and Zhou, Y. (2021). A de novo transcriptome assembly of *Ceratopteris richardii* provides insights into the evolutionary dynamics of complex gene families in land plants. *Genome Biol. Evol.* 13, evab042. 10.1093/gbe/evab042.